Experimental investigation of water absorption in polymer-matrix composite structures

SD du Plessis

orcid.org/ 0000-0002-0254-5907

Dissertation accepted in fulfilment of the requirements for the degree *Master of Engineering in Mechanical Engineering* at the North-West University

Supervisor: Prof AS Jonker

Graduation: July 2022

Student number: 26128268

ACKNOWLEDGEMENTS

I would like to thank and acknowledge my supervisor, Prof Jonker, as well as Mr Van der Walt for their guidance and input throughout my studies. I also want to express my gratitude towards Jonker Sailplanes for the use of their prototyping facilities for manufacturing the samples and supplying the materials used. I also want to acknowledge the North-West University which provided the measuring equipment and workspace for me to conduct my experimental research. A special thanks to the material lab personnel who all assisted – Mr Van Tonder, Mr Naude and Mr Diobe.

ABSTRACT

Polymer-matrix composites (PMCs) are commonly used in modern sailplanes in the primary load-bearing structure. All competition-class sailplanes make use of water ballast tanks in the wings to improve performance in certain weather conditions. Due to the adverse effects that water has on composite materials, they have to be waterproofed. There are a variety of materials that can be used to waterproof built-in ballast tanks. Yet, it is often the case that these waterproof sealants don't properly protect the underlying layers from water permeating into lower layers and being absorbed by PMCs – causing externally visible deformation.

In this study, the water absorption and permeability of PMCs used in sailplane construction were investigated. Samples were made from PMC and core foam which is used in the construction of sailplane wings. These samples were tested for **absorption** and deformation. A second set of samples made were made with coating and bonding materials (fillers) on-top of a substrate consisting of wood and fibreglass. These samples were used to measure **permeability**.

Seventeen absorption sample variants were made – each of which could be categorised according to material type for result comparison. The categories were gelcoats, fillers, fibre-reinforced composites, peel ply and PVC foam. Absorption in terms of moisture content was 0.28% to 0.29% for gelcoats, 0.50% for Novolac coating, 0.76% to 1.43% for fillers, between 1.70% and 4.88% for fibre-reinforced composite samples, 10.9% for nylon peel ply, and up to 40.7% for PVC foam. The different material samples didn't all have the same exposed surface area. It was thus necessary to implement a set of criteria to score and rank the different materials by taking the differing surface areas into consideration in conjunction with the moisture content.

Similarly the permeability experiment results were categorized in the groups of coating materials (which included gelcoats, Novolac, fluorinated plastic and peelply), PVC foam and fillers. Serving as a point of reference, permeability moisture content of the substrate-only control samples was found to be 3.58%. Two-layer peel ply samples had slightly more at 3.63%. Single-layer fluorinated plastic samples gained 3.56% moisture. Triple-layer Novolac coated samples had 3.21%. PVC foam samples had 2.12%. Triple-layer gelcoat samples ranged between 1.72% and 2.03%, and samples coated with filler materials ranged between 0.61% and 1.77%. These moisture content recordings, however, included moisture gain from moisture in the air that didn't have to pass through the materials – thus influencing the validity of reporting on these as permeability values. A permeability rank-

scoring system, akin to the one used for absorption data, was devised to take atmospheric moisture into account.

Evaluation of overall suitability of materials in aqueous environments was then done by jointly considering absorption and permeability characteristics of materials. Materials were compared within two functional, positional categories – fillers and coatings, and PMC’s and foam.

KEY TERMS

Polymer-matrix composites (PMCs), Water absorption, Water permeability, Sailplane, Gravimetric method

TABLE OF CONTENTS

TABLE OF CONTENTS (CONTINUED)

LIST OF FIGURES

LIST OF FIGURES (CONTINUED)

LIST OF TABLES

NOMENCLATURE AND SYMBOLS

Symbol/ Acronym	Description	Unit	Ref
t	Time	[h]	(Eq 1)
m	Mass	[g]	(Eq 1)
m_0	Original/initial sample mass before start of experiment When referring to a variant type, this is a 95th percentile (not an average) value of the original mass of all valid, same-variant samples	[g]	(Eq 1) Table 6
Δm	Moisture/mass gain	[g]	(Eq 1)
M	Moisture content percentage	[-]	(Eq 1)
S	Substrate of permeability sample consisting of 3 mm MDF and 6L 92125 Glass	n/a	Table 4
#L	Material layers, preceded by number (#) of layers of specified material	n/a	Table 4
D	Diameter of disc-shaped sample	[mm]	Table 4
h	Thickness of sample	[mm]	Table 4
[A]	Pertaining to absorption data	n/a	(Eq 4)
[P]	Pertaining to permeability data	n/a	(Eq 16)
δ	Measurement uncertainty		
β	Wet-to-dry moisture content ratio of a specific permeability variant	[-]	(Eq 8)
α	Ratio of dry permeability variant moisture content to the dry substrate-only (92125 Glass) control sample moisture content	[-]	(Eq 9)
γ	Ratio of wet mass gain of a specific permeability sample variant to the wet mass gain of the substrate-only (92125 Glass) variant at a specific time	[-]	(Eq 10)
Π	Rank-score; a value unique to a absorption or permeability variant	[-]	(Eq 11)
A_{exp}	Exposed (wetted) surface area of sample	[mm^2]	(Eq 18)
θ	The mass gain during wet testing per unit exposed area	[g/ mm^2]	(Eq 18)
PMC	Polymer-matrix composite	n/a	Ch 1
ct	Coating of non-control, permeability samples	n/a	(Eq 4)
w	Pertaining to permeability data from wet test	n/a	(Eq 4)
d	Pertaining to permeability data from dry test	n/a	(Eq 4)
ISO	International Organization for Standardization	n/a	Ch 3.7
gsm	Grams per square meter	[g/m^2]	Table 12

1 INTRODUCTION

1.1 Background

Many competition sailplanes make use of water ballast systems for improved performance in certain weather conditions (Federal Aviation Administration, 2013). Some sailplanes use water bags while others have integrated ballast tanks (DG Flugzeugbau, 2017).

Since a majority of high performance sailplanes are made from composite materials, those with integrated ballast tanks have to be waterproofed with some form of sealant coating to protect the composite structure from the adverse effects of water absorption (Federal Aviation Administration, 2013; Newill *et al.*, 1999). Swelling of the composite, reduced glass transition temperature of the resin, decreased structural strength, resin plasticization are some of the most notable drawbacks associated with ingress of moisture (Li, 2000). Most of these occurrences influence structural integrity and by implication, can impact the safety of the aircraft.

Apart from the reducing mechanical strength, aerodynamic efficiency can also be impaired when composites are exposed to moisture. Swelling in a composite structures changes the surface contour of sailplanes' aerofoils. Small surface imperfections on a sailplane's exterior surfaces often bring about large disturbances in airflow (Boermans & Selen, 1981). Slight deviation from the intended design, can result in undesirable aerodynamic characteristics and decreased performance.

In the wing housing the ballast tanks, sandwich composite structures (as represented in Figure 1) are used due to their high strength-to-weight ratio (Krzyżak *et al.*, 2016). Preventing water absorption within the sandwich composite structures comprising the water ballast tanks has been a challenge for a number of sailplane manufacturers (Bosman & Jonker, 2019; DG Flugzeugbau, 2017)

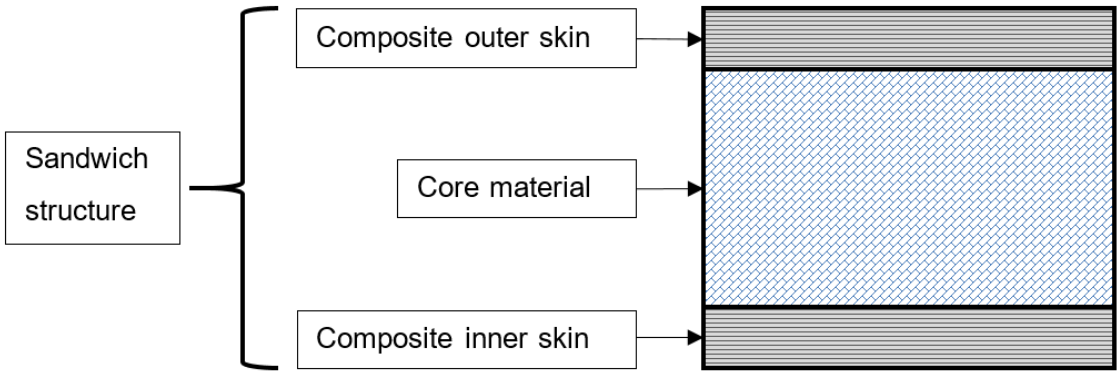

Figure 1: Diagram of a composite sandwich structure

If leaks are detected in the ballast tank, it has been unofficially recommended that the ballast tanks be “sloshed” with a liquid sealant, but this can have other side-effects such as shrinkage of the inner skin (Giddy, n/a). It has also been shown that some sealant materials are not as good as others in preventing water ingress to underlying composite materials. However, low diffusivity and solubility of a polymeric coating substance alone don’t guarantee protection against water transmission. The coating must be of good quality and sufficient thickness in order significantly slow down the diffusion process (Newill *et al.*, 1999).

At Jonker Sailplanes the integral water ballast tanks are sealed with an epoxy coating (Novolac). A brief investigation found that the coating is not effective in filling up all pinholes. The pinholes, visible as a speckled finish appear shown in Figure 2, form miniature pathways for water ingress to the underlying carbon fibre layers. Pinholes form as coating penetrates the pores on the surface of the carbon fibre surface. As an alternative to the Novolac, fluorinated plastic was used as sealer in the water tank area – unfortunately with similarly insufficient water ingress protection.

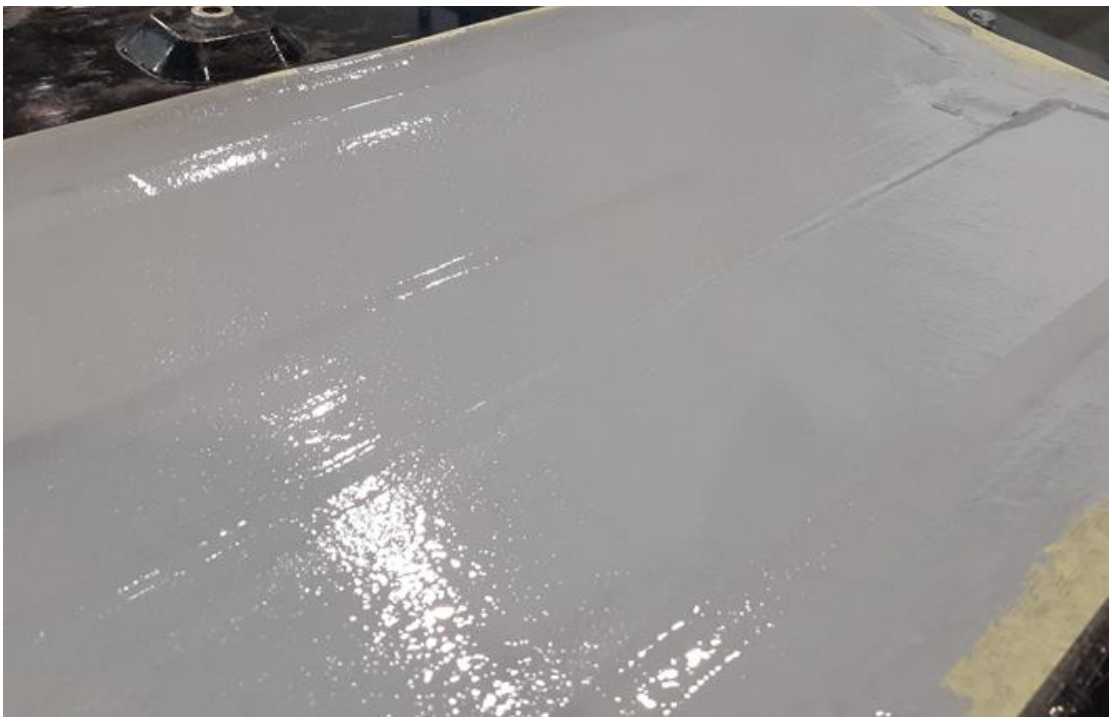

Figure 2: Speckled finish of a double-layered Novolac epoxy coating

According to Kotze (2019) the issue of water absorption within the sandwich structure is observable sometime after filling and draining the ballast tanks. Not much information has been gathered on the specific conditions the wing is subjected to prior to the distortion being noted, nor is there precise record of the passage of time before the deformation becomes visible in each incident (Grundling, 2019; Kotze, 2019). Moisture ingress in the ballast tank region of the sandwich structure is evident in the form of visible deformation on the top skin of the wing tips (Bosman & Jonker, 2019), as shown in Figure 3. It is evident upon inspection of the wing tips that the indented strip lies directly above where a structural spar is bonded to the inner skin of the composite sandwich.

Figure 4 shows a diagram adapted from CAD drawings of the wing tips. It shows a cross-sectional view of the components comprising the ballast tank region of the wing tip. This sketch is only a diagrammatic representation of the wing and some thickness and sizes have been altered for better visual clarity.

Numerous studies have been done to investigate the negative effects of moisture ingress on the mechanical integrity of sandwich composite structures (John *et al.*, 2011; LaPlante *et al.*, 2005; Manujesh *et al.*, 2014). Studies such as the one by Newill *et al.* (1999) have been done to determine effectiveness of different waterproof coatings. Various methods, each replete with their own unique equipment, have been developed to detect moisture ingress in composite structures (Giguere, 2000b). There is thus no lack of literature on water absorption.

A gap in information exists due to material specification sheets lacking comparable data. Many material manufacturers don't provide quantitative absorption characteristics. Some specification sheets do specify water-related properties, but it will often employ vastly different test methods and/or conditions (see Section 2.2.3). In other instances the specified absorption properties were determined using the same testing standard and conditions, but those laboratory-specific conditions often vary greatly from the intended, real-world application conditions.

The rational solution to address such a deficiency in data was to gather empirical data on the relevant materials by means of experimentation under the same realistic environmental conditions. This experimental study is focused on developing and investigating the use of a simplified method for quantifying moisture absorption and permeability with regards to some common materials used in polymer-matrix composite (PMC) manufacturing, specifically in a sailplane's ballast tank.

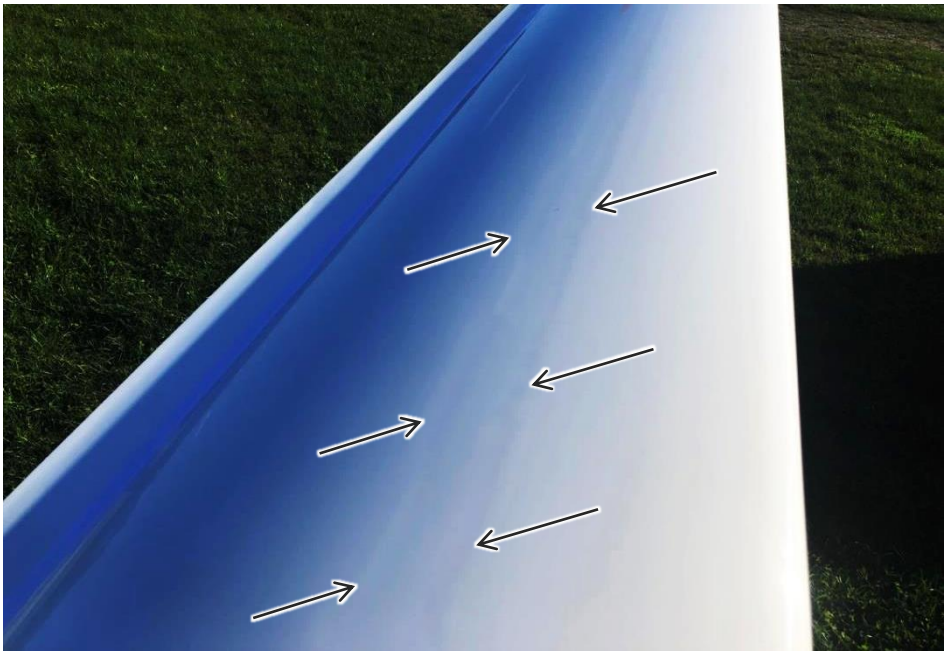

Figure 3: Swelling and/or shrinking in wing skin visible as indent along contact area of structural beam (Eisele, 2019)

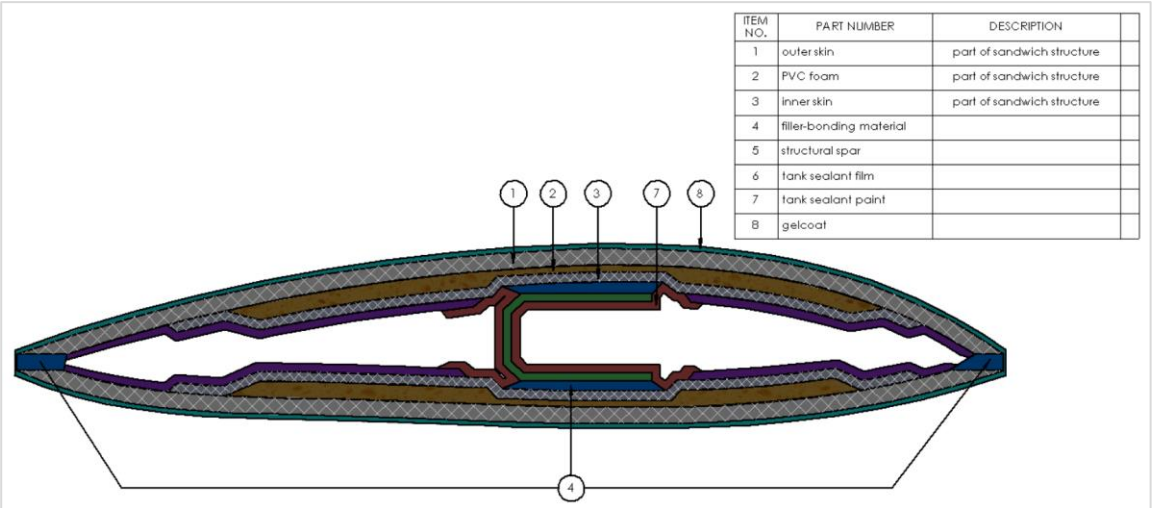

Figure 4: Diagram of the cross-section of a wing tip showing the various layers and basic components

Problem Statement

The water absorption rate and permeability of the materials typically used in the construction of sailplane wings are unknown.

1.3 Objectives

1) Use simplified experimental methods to obtain quantitative data to determine the relative water resistance of various composite materials.
2) Measure the change in thickness of test materials during testing in order to determine which materials are causing the deformation
3) Process the water absorption and permeability data to deliver a verdict on which of the tested materials best meet the requirements of low permeability and absorption.

1.4 Layout of Study

Chapter 2: Literature review of topics relating to water absorption and techniques used to quantify and detect it.

Chapter 3: Discussion and explanation of experimental methods used to carry out the experimental investigation. Sample manufacturing details are also given.

Chapter 4: Data processing

Chapter 5: Results and findings from experimental testing

Chapter 6: Conclusions and recommendations for future work on this topic

2 LITERATURE REVIEW

2.1 Introduction

The study of water absorption characteristics in PMCs started as early as the 1950s when the detrimental effects of water absorption were observed (Beaman & Cramer, 1956; Enderby, 1955). Since then much progress has been made in determining the mechanics and driving factors of absorption and permeability. Absorption behaviour models have also been created to predict different material types' absorption over time. Various techniques have also been developed for detecting and empirically quantifying water absorption and permeability.

The most commonly used method for quantifying water absorption and permeability has been the gravimetric method, since it is used by standardization organizations such as ISO (Munoz & García-Manrique, 2015) and ASTM (Gopi *et al.*, 2019). These standardized methods are often used when material manufacturers report on the water absorption properties in specification sheets as will be shown in Section 2.2.3.

This chapter evaluates the suitability of some of the typical experimental methods. Data and models from literature will be discussed as well to serve as a reference point for validation of the data obtained in this study.

2.2 Water absorption behaviour and properties of materials

2.2.1 Interaction of water with materials

This study deals with quantifying the interaction between water and materials used in glider wing construction – absorption and permeability. Moisture absorption in either vapour or liquid form has to do with the capacity of a material to absorb moisture from its environment (Ensinger Plastics, 2021). Alternatively absorption can be described as a condition in which something takes in another substance (McMurry & Simanek, 2003). Permeability characteristics of external coating materials are integral to this study as it pertains to the ability of water, under pressure, to pass through materials (McGrath, 2000). A material with high permeability allows more liquid to pass through it.

Absorption and permeation processes are driven by many of the same processes such as diffusion, polymer relaxation, hydrolysis and osmosis (Derrien & Gilormini, 2009; Gopu, 2012a). They are also influenced by many of the same factors – including temperature gradient (Bonniau & Bunsell, 1981), hydrostatic pressure (López *et al.*, 2016), porosity characteristics (Anatoly *et al.*, 2020; Choudalakis & Gotsis, 2012a;

McGrath, 2000), relative humidity and material thickness (Newill *et al.*, 1999). Since temperature is not a controlled variable in this test, it is useful to note the influence of temperature differences on moisture absorption. A study conducted by Suh *et al.* (2001) on identical carbon fibre samples at different temperatures showed that a 25°C increase in water temperature only lead to a 4% increase (relative to absorption at 35°C) in moisture absorbed at equilibrium.

However, by the differences in definition of what these processes entail, it is possible for permeability and absorption to be opposite for a certain material or combination of materials. For example, a perforated, hydrophobic membrane can allow water to pass through it freely due to the large, continuous pores (resulting in high permeability), yet very little moisture can be taken up into the material itself (resulting in low absorption). The inverse is also possible. A material with discontinuous pores can allow very little liquid water to pass through it (low permeability), but absorb a significant amount of water in its surface layers – only allowing water to pass through after an extensive duration of exposure to water (Maxwell *et al.*, 2005).

This investigation, although related to PMCs subjected to contact with liquid water in the ballast tank, the effects of water vapour cannot be excluded. Due to its very small molecular size, water vapour will nearly always pass through laminates, albeit in small quantities (Bumgarner, 2003; Gurit, 2021; Wong, 2013). As a result of this nearly inevitable form of water ingress, materials are often made to be both waterproof and breathable. This is done so that material can dry more efficiently once removed from the marine environment, or in the case of a ballast tank, once the water has been drained from the tank. A diagrammatic illustration of waterproof breathability of a material is shown in Figure 6. Increasing drying efficiency is important since the amount of degradation done by moisture ingress is directly proportional to the duration of exposure (Weitsman, 1991). Ensuring maximum water desorption is crucial in preventing irreversible degradation effects (Antoon & Koenig, 1980; Wong, 2013).

Another factor of interest is that PMCs tend to absorb more moisture and offer lower water permeability resistance upon repeated cycles of testing under the same environmental conditions according to a study conducted by Tsenoglou *et al.* (2006). This is significant as this study involves experimental tests conducted repeatedly over several rounds with the same samples.

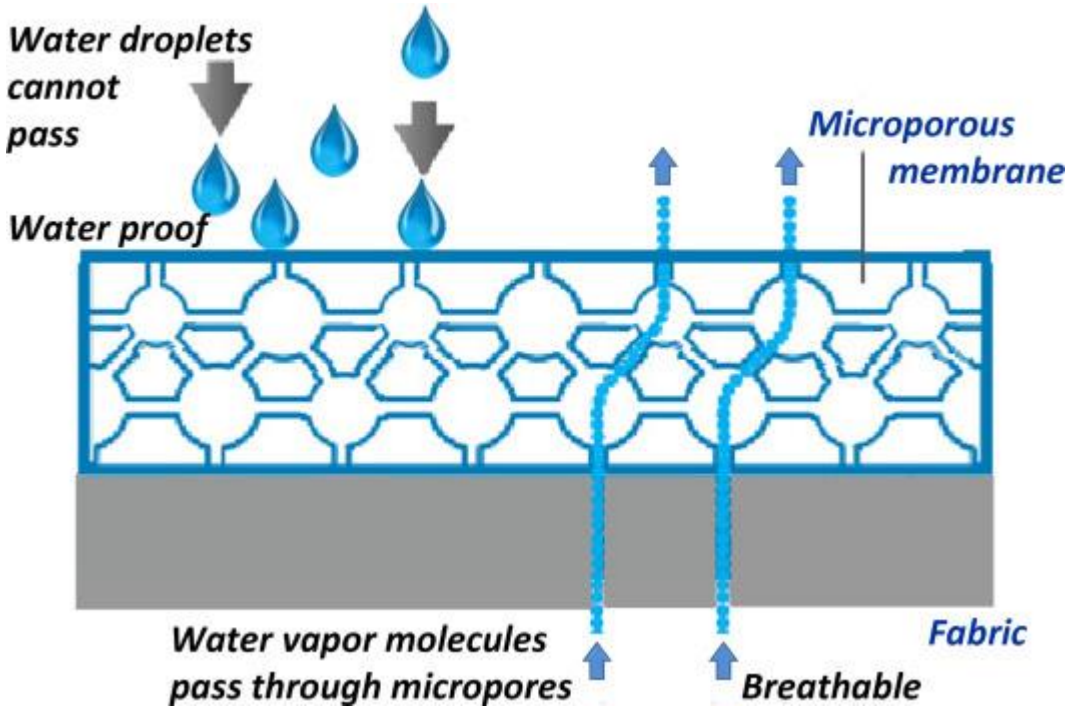

Figure 5: Diagram **of how suitably-small sized pores in a membrane can waterproof an underlying layer of fabric while providing breathability**(Özek, 2018)

2.2.2 Predicted behaviour

This section deals with some predicative models and tendencies of water absorption in materials as determined in other studies. These models and behaviour classifications show how materials typically absorb water over the course of time. Understanding the absorptive tendencies of materials helped improve the methodology, particularly how frequently readings had to be taken to accurately plot a material's absorption over time.

A good departure point in understanding absorption and permeability behaviour was to become acquainted with general mechanisms involved in diffusion. Diffusion is often a central point in absorption studies because it is the primary mechanism by which both absorption and permeation occur (Gopu, 2012a; West, 2021). Based on numerous absorption experiments conducted on polymer systems over decades, at least four general types (shown in Figure 6) of behaviour for diffusion were identified (Alfrey Jr *et al.*, 1966; Hopfenberg & Stannett, 1973; Park & Crank, 1968; Rogers, 1965). Diffusion of water in polymers has most often been assumed to be constant before approaching saturation point in a wide range of investigations (Shirangi & Michel, 2010). This generally-assumed behaviour is known as Fickian diffusion (Gopu, 2012b). Contrary to Fickian behaviour, studies conducted by Apicella *et al.* (1983) and Grammatikos *et al.* (2015) illustrated that there is often a mass loss effect as shown in Figure 7. This can

be attributed to chemical decomposition of material when exposed to water which influences gravimetric mass measurements. This leads to another deviation from the standard Fickian diffusion.

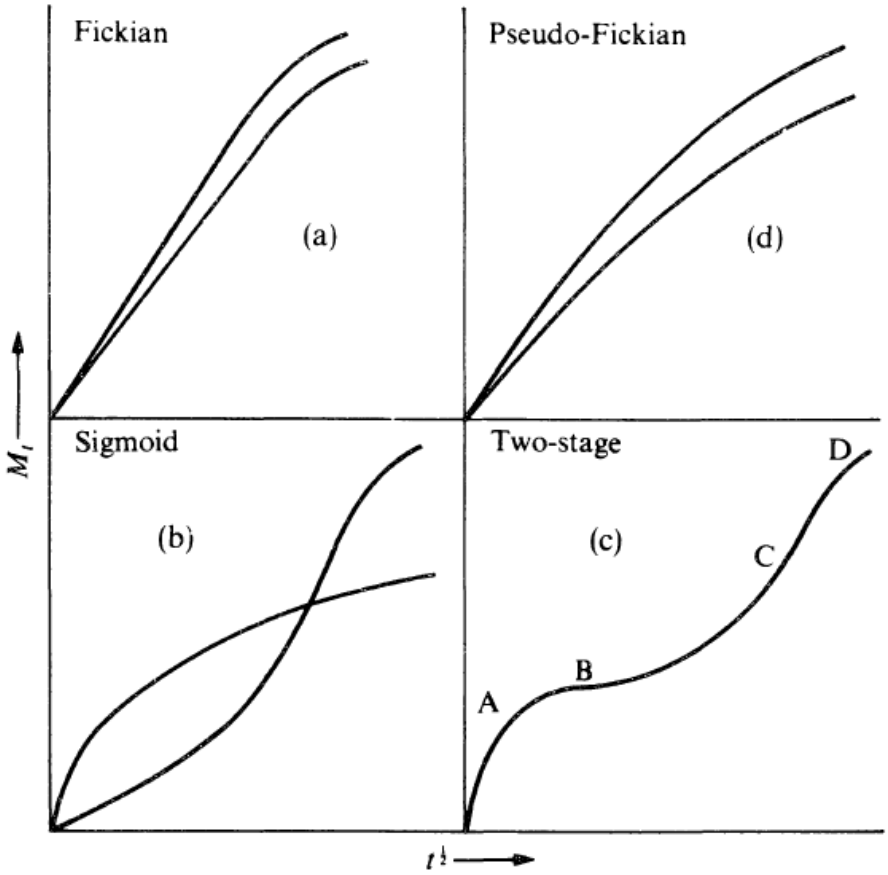

Figure 6: Four Fickian diffusion curve types (Rogers, 1965)

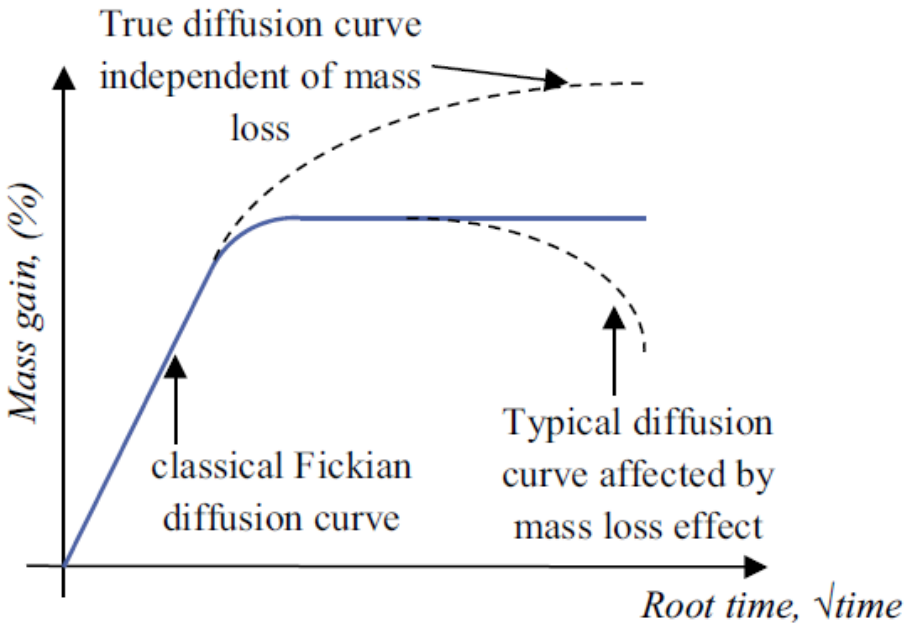

Figure 7: Variations of Fickian diffusion (Grammatikos *et al.*, 2018)

A study by Surathi and Karbhari (2006) conducted on vinyl ester specimens using the gravimetric method showing the influence of water temperature on absorption. Figure 8 displays the curves of specimens' moisture absorption over 1500 days. When looking at the shorter timespans (less than 30 days), it can be seen in the graph that the effect of temperature becomes significantly less with shortened timespans. The difference between 23°C and 40°C at 30 days is less than 0.03%. This is important to note as the investigation done on PMCs in this paper looks at comparing materials' absorption after an even shorter period of 300 hours (less than 13 days). Inspecting this short, initial timespan of the study conducted by Surathi and Karbhari (2006) is of interest because it more accurately represents the shorter durations that sailplane tanks are typically filled with water before being drained within 20 hours. Even in instances of exceptionally long, speed record flights, continuous journeys don't exceed 15 hours (Clément, 2006). The reason for surpassing the realistic 20-hour water exposure by 280 hours was to avoid the larger measurement uncertainty associated with smaller changes in mass. Additionally, materials are often still absorbing at similarly high rates within the first 100 hours, making it harder to differentiate their absorption and permeability characteristics. Selecting 300 hours as the benchmark time served as a suitable compromise between realistic exposure duration and materials approaching the saturation point, where it is easier to distinguish material performance.

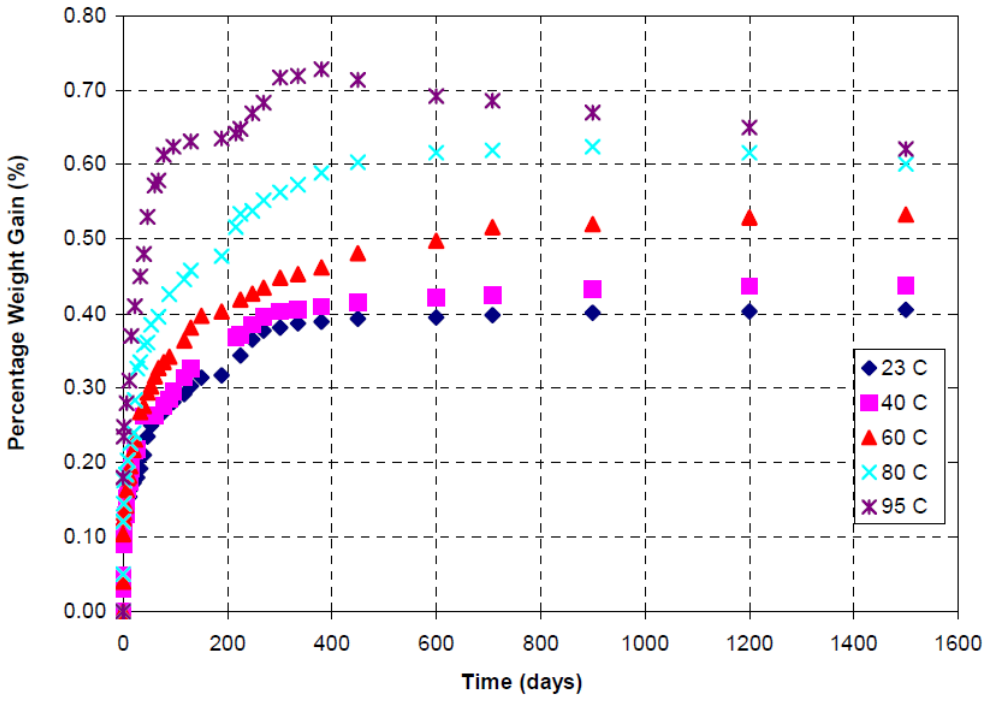

Figure 8: Moisture gain of vinyl ester specimens submerged in water at varying temperatures(Surathi & Karbhari, 2006)

Another interesting observation was made in a study by Monson *et al.* (2008) on polyamide plaques. This particular study found that the variation in sample thickness had very little effect on the mass absorption ratio (m/m_0). Thickness (B_0) variation could, however, significantly influence how quickly saturated mass was reached (refer to Figure 9).

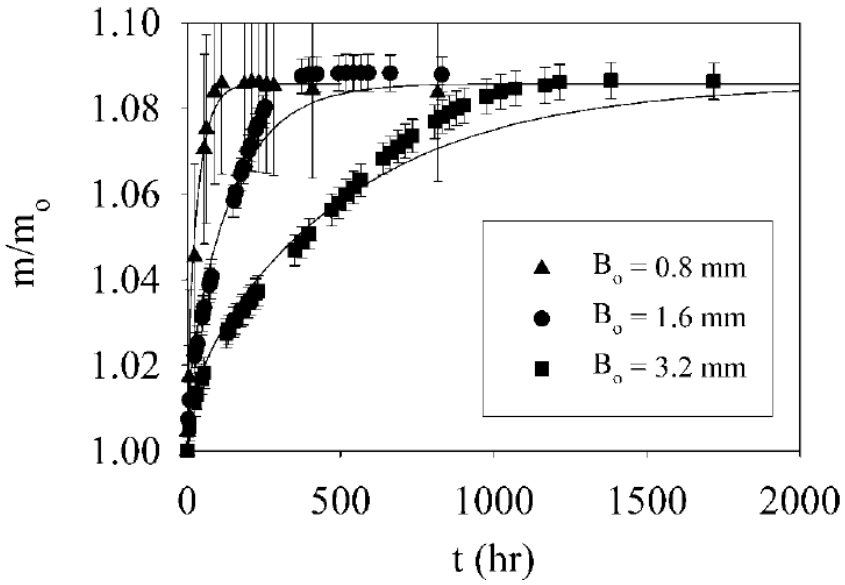

Figure 9: Mass absorption ratio versus time for polyamide plaques of various thickness (Monson *et al.*, 2008)

2.2.3 Available information on material characteristics

Specification data sheets of composite materials usually give very little information on the absorption and permeability characteristics – if any. Of the thirteen materials selected for this study, only two datasheets provided absorption data. An alternative way to obtain some information was to look at the data for similar materials. Table 1 lists the alternative material data found. Nonetheless, data could not be found for any of the filler materials (cotton flocks and fumed silica/Cab-O-Sil®). Another source of difficulty is that none of the datasheets specified the test standard used. Only two studies reporting absorption values using identical test conditions, namely ASTM D570 for 90070 Glass and polypropylene. This made the comparison of absorption data, based on literature alone, virtually impossible.

Data for permeability of water through PMC's was even scarcer than for absorption. Permeability tests were most often conducted to measure the permeability of water vapour and not liquid water through a material (Anatoly *et al.*, 2020; Keller & Kouzes, 2017), as was desired for this study. Consequently, a simple and novel testing method

was developed (as will be explained in Section 3.3) for permeability testing which allowed for the direct comparison of data for the materials of interest.

Table 1: A list of the absorption data obtained for similar type materials in other studies

	Similar Type Material/External Study of Test Material					
Test Material Name	**Name of Similar Material**	**Absorption Value**	**Duration [h]**	**Temperature [°C]**	**Test method standard**	**Reference**
Carbon 9001 MDL	Carbon fibre epoxy resin pre-preg	1.4%	-	-	-	(Zhai *et al.*, 2016)
Carbon 98141	UD carbon with epoxy resin	0.8%	300	23	-	(Arnold *et al.*, 2012)
92125 Glass	E-glass with vinylester resin	0.370%	288	23	-	(Surathi & Karbhari, 2006)
90070 Glass	glass fibre with vinylester resin	0.57%	294	45	ASTM D570	(Gopi *et al.*, 2019)
	E-glass with isophthalic polyester resin	0.9%	300	60	-	(Grammatikos *et al.*, 2018)
MDF	Medium density fibre board (MDF)	80%	168	23	ASTM D 1037?	(Xu *et al.*, 1996)
Polypropylene	Polypropylene	0.01%	24	23	ASTM D570	(Sterling Plastics, 2012)
Cotton flocks	-	-	-	-	-	-
Cab-O-Sil®	-	-	-	-	-	-
Peel Ply	Polyamide 6	8.6%	370	25	-	(Monson *et al.*, 2008)
	Polyamide 6	9%	-	-	-	(Raghavalu Thirumalai *et al.*, 2011)
Rhino 9700	**Rhino 9700**	<1%	-	-	-	(Rhino Linings, 2020)
Gurit PVC60 Foam	Airex® C70.55	**0.15mg**[1]	168	23	DIN 53428	(Airex AG, 2010)

2.3 Water absorption detection methods

The degree to which water penetrates materials in a structure can be observed by employing various techniques – some destructive, some non-destructive (requiring that

[1] Moisture content percentage not given and sample mass unspecified.

the structure be cut open to expose the affected region). Each technique is limited to detect specific stages or types of moisture-related damage, ranging from mere moisture penetration to corrosion (Giguere, 2000a). Detecting distribution of absorbed moisture within a structure without cutting the structure open is possible with the right equipment. However, many of these non-destructive techniques such as infrared thermography, radiography and helium mass spectrometer leak detection require very costly equipment.

Two particular methods were identified as viable for this research, namely the gravimetric method and the electrochemical impedance spectroscopy, or EIS, technique.

The gravimetric method for determining moisture-related properties of materials has been commonly employed by many researchers (Heydari & Sheibani, 2015; Surathi & Karbhari, 2006). Gravimetric methods entail the physical measuring of a sample's mass at specific time intervals to determine what change in mass (Δm_t) occurred in the presence of moisture usually expressed as a percentage (M_t) relative to the initial mass (m_0).

$$M_t[\%] = \frac{\Delta m_t}{m_0} \times 100 = \frac{m_t - m_0}{m_0} \times 100 \qquad \text{(Eq 1)}$$

Although not without limitations and drawbacks, this method is intuitive, simple, and relatively cost-effective and has been used in international, standardized absorption testing methods such as and ISO 62:2008 (Munoz & García-Manrique, 2015; Zarski *et al.*, 2020). One such negative aspect of the gravimetric method is that before being weighed, samples have to be withdrawn from the source of moisture and then be partially dried to remove surface water, since this moisture has not yet been absorbed by the sample (Grammatikos *et al.*, 2018).

Unlike the gravimetric method, the EIS technique negates the need for removing the sample from the moisture source (Grammatikos *et al.*, 2018). EIS is a useful non-destructive method which uses digital impedance measurements to quantify changes in sample composition. Low-cost versions of the EIS system have been developed (Grassini *et al.*, 2014). However, the method is complex in terms of calibration (which does require gravimetric data on the samples anyway), setup of the various intricate components, signal noise and null corrections (Hsieh *et al.*, 1995).

In this study the gravimetric method will be used due to its lower complexity and acceptance as a proven method.

2.4 Data processing techniques

Due to the nature of processing large amounts of readings from multiple samples of each material, it was necessary to employ some basic data processing methods.

Cumulative effects of measurement uncertainty in values of parameters involving these measured variables could be determined by means of the standard error propagation rules and their associated formulas. Although these rules and formulas can't be attributed to a single author or entity, as their exact origin couldn't be determined, this study made use of the guidelines as given by Taylor (1997). The guidelines of interest for this study pertained to the addition/subtraction and division/multiplication rules of **dependent** variables with measurement uncertainty. The variables in this experimental investigation are **correlated**, as they are subsequent readings of the same property of the same samples. The cumulative error, $\delta \mathrm{E}$, of a variable, E, resulting from the addition and/or subtraction of dependent variables $a, b, c, \ldots$ each with uncertainty $\delta a, \delta b, \delta c, \ldots$ can be approximated with the following equation

$$\delta \mathrm{E} \leq \delta a + \delta b + \delta c + \cdots \qquad \text{(Eq 2)}$$

Likewise, the cumulative error, $\delta \mathrm{E}$, of a variable, E, resulting from the multiplication and/or division of dependent variables $a, b, c, \ldots$ each with uncertainty $\delta a, \delta b, \delta c, \ldots$ can be approximated with the equation

$$\delta \mathrm{E} \approx |E| \cdot \left(\frac{\delta a}{|a|} + \frac{\delta b}{|b|} + \frac{\delta c}{|c|} + \cdots \right) \qquad \text{(Eq 3)}$$

Practical verification calculations using these error propagation formulas are done in Section 5.6.1.

The existence of outliers was anticipated, as PMC samples would in all likelihood have defects, some of which could have significant effects on water absorption and permeability characteristics which would be erroneous to include in further calculations. The outliers could be identified using the standard method of setting up inter-quartile range limits for non-outlier data (Tukey, 1977).

2.5 Summary

In this literature review the water absorption properties of various materials as supplied by the manufacturers were investigated. It was found that limited data is available and

that various manufacturers used different test methods making a direct comparison difficult. It is therefore clear that an experimental investigation of the different material of interest using the same method will enable a direct comparison of the absorption and permeability properties.

Different test methods were also investigated and it was decided that the gravimetric method will be best suited for this study. Finally, the basic data processing methods were given that would be used to process the recorded data obtained using the gravimetric method.

3 EXPERIMENTAL METHOD

3.1 Introduction

Seeing as the gravimetric method with regards to measuring moisture content is merely a category under which many standardised methods exist, it was necessary to stipulate the specifics of exactly how the gravimetric method would be employed in order to measure two different parameters related to water ingress. This chapter provides the detailed experimental setup and procedure of absorption and permeability tests. The sample manufacturing procedure and sample particulars are also discussed. Thereafter, specifics are given on the measurement system analysis method used to scrutinise the uncertainty of the readings obtained from the specific method implemented in this study.

3.2 Experimental setup

The absorption and permeability experiments ran in parallel, so that they would be subject to the nearly the same environmental conditions. Each of the two individual experiments also required unique samples. Experiment-specific samples came in different variants respectively containing a different test material and/or having a dissimilar nominal thickness from other variants. Furthermore, several examples were made of each variant in order to obtain more data and consequently a better representative of the inter-variant spread of characteristic values. The procedure followed for each of the two experiment types is given in the following subsections (permeability in Section 3.3 and absorption in Section 3.4). Equipment and components used for both permeability and absorption are shown in Figure 10. Length and width, or diameter were measured using a digital calliper vernier, while sample thickness was determined using the micrometer. The analytical balance was used to measure mass of samples. The usage of other experimental equipment and materials are described in experimental procedure subsections (3.3 and 3.4).

The resolution and precisions of measurement instrumentation is listed in Table 2. These values were determined after executing measurement system analysis (MSA).

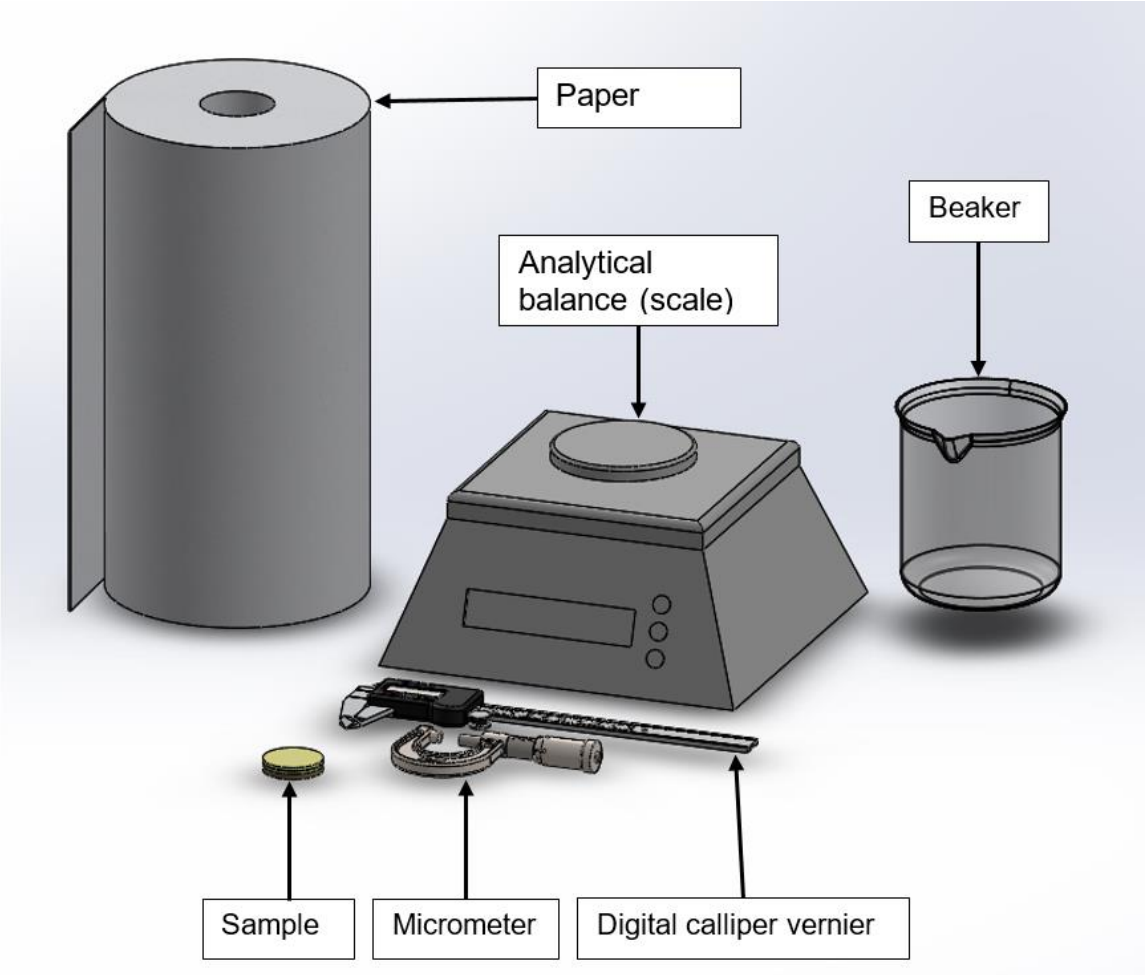

Figure 10: Diagram of instrumentation and components used for permeability and absorption experiments

Table 2: Precision and measurement uncertainty of instruments

Instrument	Resolution	Measurement uncertainty
Micrometer	0.01 [mm]	0.04 [mm]
Digital vernier calliper	0.01 [mm]	0.01 [mm]
Mass scale 1 (AE)	0.05 [g]	0.05 [g]
Mass scale 2 (Sartorius BP 110 S)	0.0001 [g]	0.0002 [g]

3.3 Permeability experimental procedure

Since water permeability pertains to the ability of water to pass through a material (McGrath, 2000), this experiment was set up to measure how much water would pass through the test material and into the absorbent substrate of a sample. This was accomplished by inserting a sample (which was weighed and had its thickness recorded beforehand) into the female PVC fitting as shown in the assembly drawing in Figure 11. The coated side of the sample faced upwards, pressing against the o-ring and the male PVC fitting was screwed on tightly from below. Coloured, distilled water was then poured from the beaker onto the top side of the sample. The time at which water was added was noted. After a specified time had elapsed, the water was poured out into the beaker. Next, the samples were then quickly dried individually with a paper towel (to remove unabsorbed surface water) and weighed within one minute of drying and the time of recording was noted. The samples were then inserted into the test rig as before and the water in the beaker was added again. This process was repeated until the final interval, upon which the thickness was also measured. The aforementioned process was repeated with the same samples for four rounds. Between rounds the samples were dried in an oven for at least 24 hours at 50°C. This was done to get the samples within 5% of their original mass (under 2% on average) – with the exception of some MDF samples that were up to 13% lighter than their original mass.

The effect of atmospheric moisture being absorbed by the permeability samples had to be quantified by placing permeability samples in the test rigs as usual, but without adding water. This waterless version of the experiment will furthermore be referred to as the dry experiment. The dry permeability experiment was carried out alongside the usual (wet) permeability testing. Dry and wet data in the rest of this report are denoted by an underscore “d” and “w” respectively.

ITEM NO.	COMPONENT NAME	QTY.
1	female PVC fitting	1
2	male PVC fitting	1
3	o-ring	1
4	sample	1
5	water	1
6	catchment seal	1

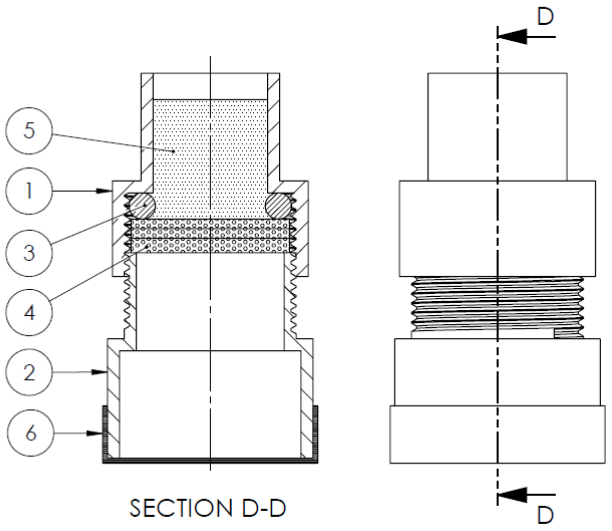

Figure 11: Assembly drawing of the components for the permeability experiment

3.4 Absorption experimental procedure

Moisture (water, either in vapour or liquid form) absorption has to do with the capacity of a material to absorb moisture from its environment (Ensinger Plastics, 2021). In order to replicate the highest possible absorption scenario at room temperature whilst having a low hydraulic pressure, this experiment's samples were totally submerged in water (filtered using reverse-osmosis to remove common impurities). This allowed for water ingress from all sides.

The adapted gravimetric procedure for this experiment started with weighing the samples and measuring their dimensions. Absorption samples of the same variant were then placed in suitably sized containers. Square samples were stacked vertically on-top of each other, with thin spacers in-between. The piles were arranged so that the water would come in-between the samples in the gap created by the spacer/seal. This arrangement prevented the surface area from being significantly reduced due to samples being sandwiched together (refer to Figure 12). Disc-shaped samples of the same variant were placed at an angle against each other without any spacers as shown in the drawing in Figure 13. All containers were then filled with coloured water until all samples

were completely covered with water. In instances where the samples had a density lower than water, small weights were placed on-top to prevent them from floating to above the water level. After a specified time had elapsed, samples were then removed from the water container and then individually dried with a paper towel and weighed within 30 seconds of drying. Weighed samples would then be returned to the container. This process was repeated periodically until the end of the test sequence. The sample dimensions were measured at the end of the test sequence. As with permeability samples, the samples were dried in an oven for at least 24 hours at 50°C between different test sequences. This was done to get the samples within 5% of their original mass (less than 1% on average). This 5% limit was only exceeded by some MDF samples that were up to 7% lighter than their original mass.

It should be noted that the difference in hydrostatic pressure between the sample at the bottom of the pile and the one at the top of the pile was between 570 and 785 Pa. It has been shown in other studies that differences in the order of 10 MPa still show small or negligible effects on water absorption in polymers (Tucker *et al.*, 1993). Significant differences have been observed with hydrostatic pressure difference in the order of 100 MPa (López *et al.*, 2016). Thus it was improbable that the hydrostatic pressure in this experimental setup would have a measurable effect on the absorption of samples.

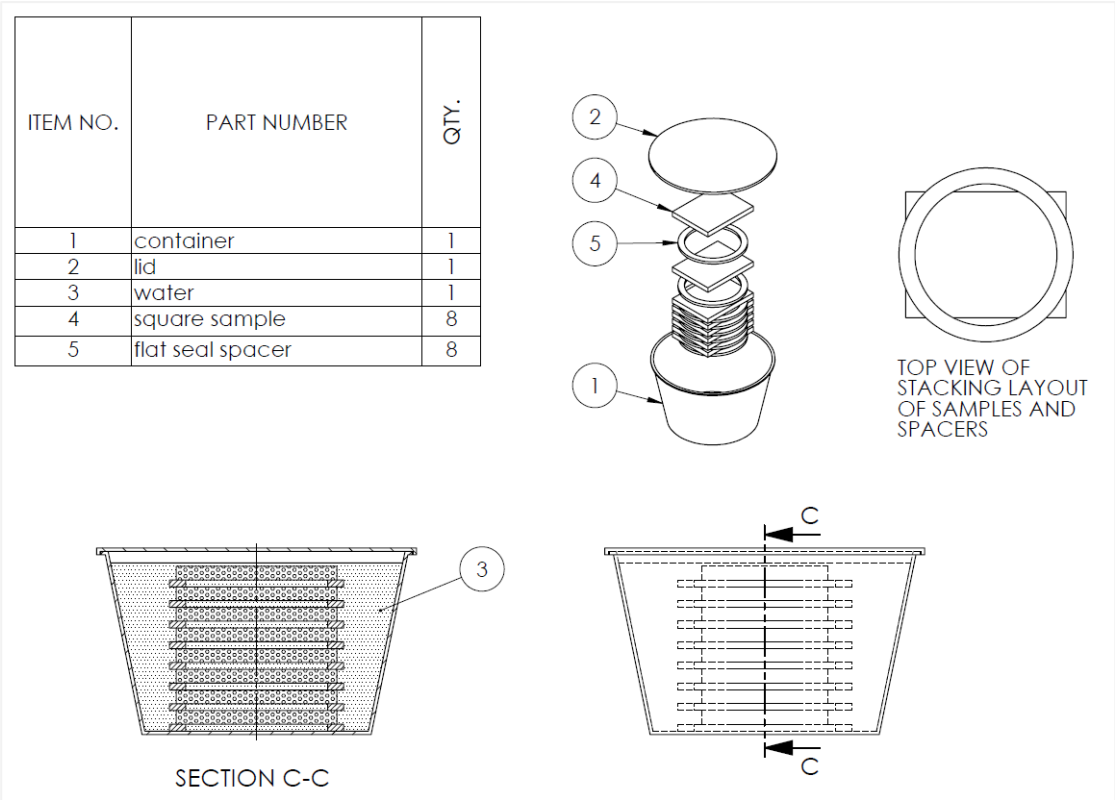

Figure 12: Assembly drawing of the components for the absorption experiment for square samples

ITEM NO.	PART NUMBER	QTY.
1	disc sample	8
2	water	1
3	container	1
4	lid	1

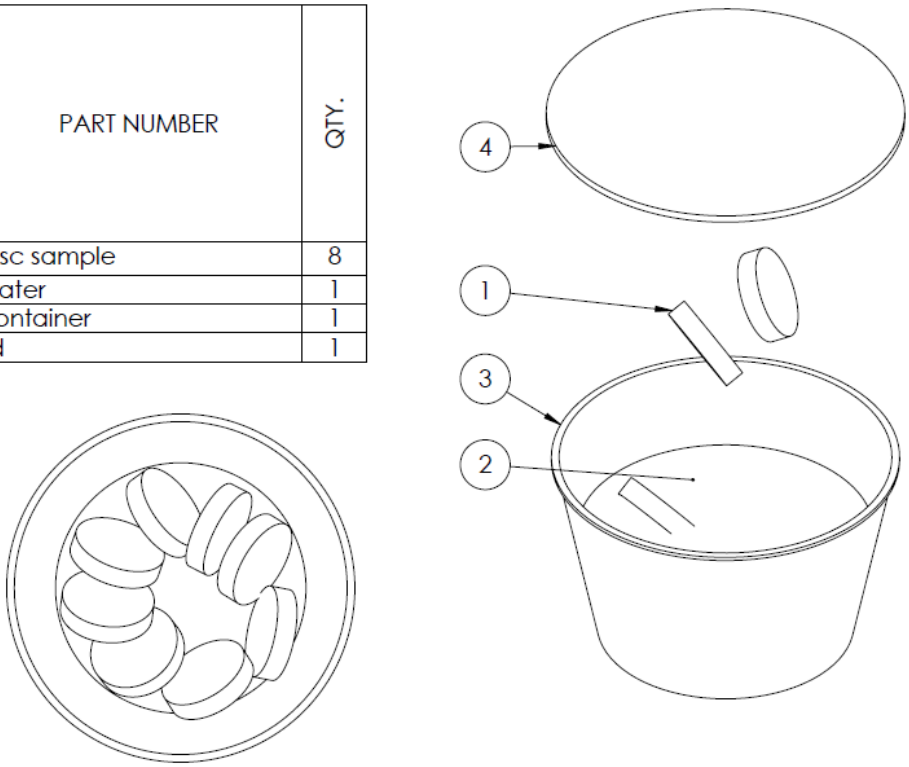

Figure 13: Assembly drawing of the components for the absorption experiment for disc-shaped samples

3.5 Preliminary tests

In order to test and sort out potential difficulties, two preliminary tests were done before the full-scale permeability and absorption tests described previously. One preliminary test tested a method to enhance the visibility of areas that absorbed water and the other tested the effectivity of the permeability experimental setup.

3.5.1 Colourant experiment

Since water generally leaves nearly insignificant traces after evaporating, a visual enhancement method was tested. The objective was to test if colouring distilled water would help trace the path of water penetration in both permeability and absorption samples. The main requirements for suitable colourants were visibility and solubility. Without solubility, the colourant will not permeate into the material along with the water –creating the false appearance of good water resistance. If the colourant is not visually distinguishable from the material itself, the test will be of no use.

Due to their high visibility, two food colourants' solubility properties were researched. The colourants were sky blue, also known as Acid Blue 9/Brilliant Blue FCF, and Crimson Pink, also known as Azorubine/Carmoisine/Acid Red 14. Research showed that the four highest occurring substances – water, colorants (E122), acidity regulator

(E330) and extra neutral ethanol – in the colouring were all highly soluble in water (Commission, 2012; Lide, 1995; Ltd, 2019; NTP, 1992). Of the two remaining ingredients, only one was slightly soluble (Lide, 1995).

An elementary visibility experiment was performed by mixing increasing concentrations of food colouring in water. It was found that the colouring dissolved completely and didn't separate into layers with time, which confirmed that the colorant is soluble (refer to Figure 14). The coloured water was then applied to the surface of Gurit® PVC60 Foam samples which were left to soak in the water and then allowed to dry (see Figure 15). The colourant remained after the water had evaporated and clearly showed where the water had penetrated the porous surface.

It was later noted in full-scale absorption testing (not the preliminary colourant experiment) with dark grey carbon samples that the colourant residue was not visible. The colourant also didn't adhere to the surface of samples coated with one of the varieties of gelcoat tested and was thus wiped off when drying the samples before weighing them (refer to Figure 16 and Figure 17). The coloured water would proceed to prove useful in detecting leaks in permeability testing rigs of all the other samples as well as providing a visual indication of water penetration depth. Acid Red 14 was used in full scale testing since it provided better contrast than the Acid Blue 9 on a greater variety of test materials.

Figure 14: Red colourant dissolving in distilled

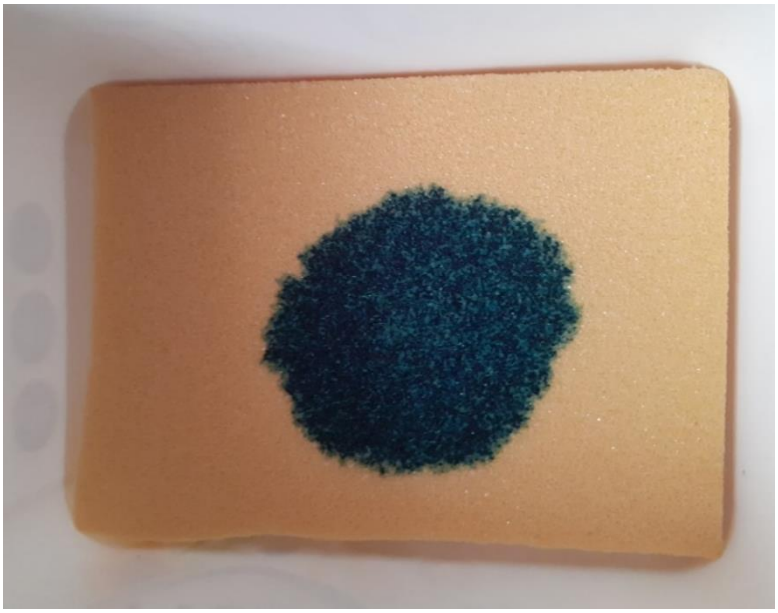

Figure 15: PVC60 Foam sample with residue from blue colourant remaining

Figure 16: GC 253PA retained no residue of the red colourant

Figure 17: The colourant adhered to the surface of GC 1 050

3.5.2 Permeability screening test

The main purpose of this test was to test the permeability experiment's intended setup before starting full-scale testing. The samples made for this test were used exclusively in this experiment. The permeability experimental procedure outlined in section 3.3 was followed. Data from this test was solely used for screening and trial purposes. Consequently, data acquired from this preliminary experiment is **not** included in the Section 5. RESULTS .

The samples were manufactured by the same process to be described in Section 3.6.3, albeit without the MDF layer and a thinner 92125 Glass component (two layers instead of six). These screening samples weren't trimmed as precisely as the full-scale permeability samples. This had the effect that some screening samples failing to seal properly against the o-ring (see Figure 18).

It was discovered during this screening test that simply two layers of 92125 Glass with a coating material presented some flaws. The first problem was that the two layers of Glass 92125 remained quite porous — porous enough for water to pass through easily (as shown in Figure 19). The second drawback was that there was no way to know how much water had permeated through the coating material, since the 92125 Glass layers would retain very little moisture and water that fell into the catchment seal would also partly evaporate or leak through. These problems were addressed by adopting a different design for the full-scale permeability samples – as described in Section 3.6.2 below.

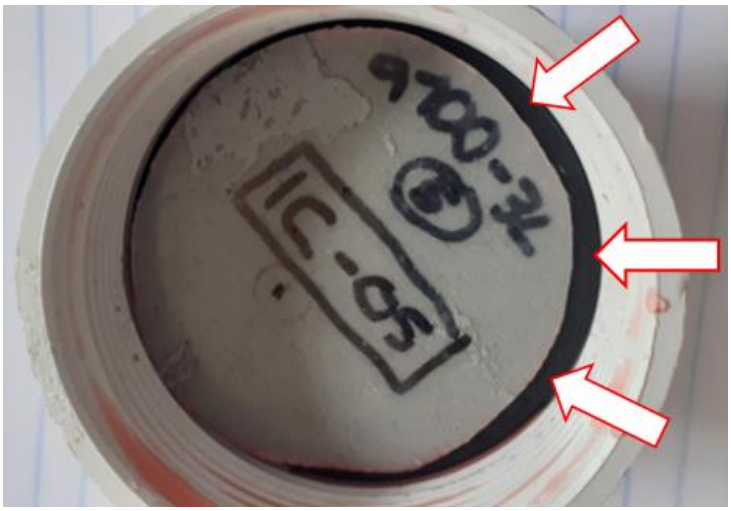

Figure 18: Preliminary sample that was cut too small. Black o-ring is visible along short side.

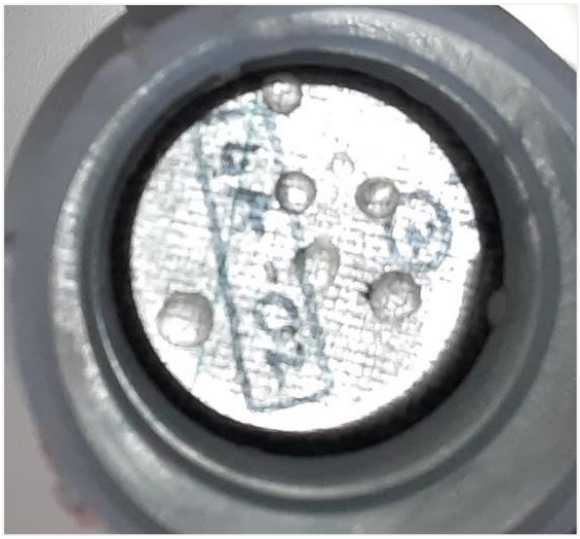

Figure 19: Droplets seen forming as water penetrates downward through pores of the preliminary sample

3.6 Materials and manufacturing

The primary materials which make up and are used to waterproof the ballast tank region of a JS3 Sailplane were used to make samples. Several materials were added for reference purposes. The different materials tested for absorption and permeability are listed in Table 3. Based on a combination of the material make-up, location and function, three categories were made for comparing related materials. The comparison categories were:

1) Fillers and coatings,
2) PMCs and foam (core material), and
3) Control

3.6.1 Material categorical traits

Fillers and coatings were the materials that surrounded the sandwich structure described in the introduction. The gelcoats were applied on the outside of the structure while fillers, fluorinated plastic and epoxy Novolac were used on the inside of the ballast tank. This meant that gelcoats did not actually make direct contact with the water in the ballast tank, but these coating materials were still tested as alternatives. All these materials had some role to play in protecting the underlying structure from water ingress, so they were tested for both permeability and absorption. Fluorinated plastic was the only coating material not tested for absorption. A secondary objective was to obtain deformation data on these materials.

PMCs and foam comprised the actual sandwich structure. Neither of these two material types were intended to make direct contact with water. Water permeability was not a practical concern with the materials in this category, since their function was not to prevent water ingress. However, quantifying the water absorption capacity of these materials would provide insight to the amount of water absorbed by individual structural materials if water did penetrate through the surrounding layers of fillers and coatings.

Lastly there were control materials, namely polypropylene and medium-density fibre board (MDF). Polypropylene was selected due to its low water absorption characteristics (Deng *et al.*, 2010). In contrast, MDF was selected for its high absorption properties. These two materials were selected to form high and low reference points for non-control materials in terms of absorption.

Table 3: Details of test materials used in absorption and permeability experiments

Material	Category	Material Description
Cotton flocks	Filler	Mixture of epoxy, cotton flocks (milled cotton fibre) and CoS in a mass ratio of 20:3:1
Cab-O-Sil® (CoS)	Filler	Consists of a mixture of epoxy and CoS (fumed silica) in a mass ratio of 10:1
Rhino™ 9700	Coating	Also known as “Jeffco” Paint-on epoxy Novolac coating and lining system
Fluorinated plastic	Coating	Thin sheet applied to epoxy-wetted surface
Peel Ply	Coating	Porous polyamide release fabric wetted-out with epoxy
Scott Bader Crystic® GC 253PA	Coating	Epoxy bonding gelcoat resin used with Andonox KP-9 Hardener
SikaBiresin® GC050 (GC 1 050)	Coating	Epoxy gelcoat resin used with GC 11 hardener
Carbon 98141	PMC	200gsm, 2/2 Twill weave carbon fibre fabric
Carbon 9001 MDL	PMC	140gsm, plain weave carbon fibre/fibreglass hybrid fabric wetted-out with epoxy
90070 Glass	PMC	80gsm fibreglass fabric wetted-out with epoxy
92125 Glass	PMC	280gsm fibreglass fabric wetted-out with epoxy
Gurit® PVC60 Foam	Core material	5 mm thick, closed cell, cross-linked polyvinyl chloride (PVC) foam
MDF	Control	Highly absorbent Homogenous panel of bonded wood chips Control material
Polypropylene	Control	Highly resistant to moisture absorption Control material

3.6.2 Sample composition and attributes

As mentioned in the Section 3.2, permeability and absorption samples differed in composition (refer to Table 4). The sample composition of samples discussed in this section exclude the unique samples made for the preliminary testing discussed in Section 3.5.

Non-control permeability samples consisted of a test material component and a substrate underneath. The substrate consisted of six layers of 92125 Glass on-top of a 3 mm MDF layer. The 92125 Glass served as an application-realistic PMC surface for the test material to be applied to. The MDF served as a highly absorbent catchment material. Consequently, any significant percentage of water permeation through the upper layers reflected as a sudden mass increase. The sample area exposed to water was nearly identical (within 10%) for all permeability samples since they were all disc shaped with a diameter of 56±2 mm and only varied in thickness (which did not affect the exposed area).

Absorption samples consisted solely of a test material. Sub-variants of certain materials were manufactured to test the effect of thickness and area-to-volume ratios. Absorption samples were generally thin, square-shaped specimens, but all the casted variants were disc-shaped. Table 4 also lists the shape, average thickness and surface area of the various absorption sample variants. More on the effects of varying thickness and surface areas of these samples will be discussed in the results.

The substrate consisted of six layers of 92125 Glass on-top of a 3 mm MDF layer and is designated by an “S” in Table 4. The 92125 Glass served as an application-realistic PMC surface for the test material to be applied to. The six layers of 92125 Glass provided a less porous, more uniform surface than the 2-layered types used during screening tests. The MDF served as a highly absorbent catchment material. Consequently, any significant percentage of water permeation through the upper layers reflected as a sudden mass increase. The sample area exposed to water was nearly identical (within 10%) for all permeability samples since they were all disc shaped with a diameter of 56±2 mm and only varied in thickness (which did not affect the exposed area).

Table 4: Sample variant details for both permeability and absorption experiments

Permeability Samples			Absorption Samples			
Variant	**Composition**	**h [mm]**	**Variant**	**Shape**	**h [mm]**	**A [×10^3 mm^2]**
MDF	3 mm wood	3.1	MDF	square	3.1	7.3

Permeability Samples			Absorption Samples			
Variant	**Composition**	**h [mm]**	**Variant**	**Shape**	**h [mm]**	**A [×10³ mm²]**
92125 Glass	S	4.8	92125 Glass – 6L	square	1.3	4.6
-	-	-	92125 Glass	square	4.1	9.3
-	-	-	92125 Glass	square	5.7	9.6
Polypropylene	S+1L	6.0	Polypropylene	square	0.8	8.8
Cotton Flocks	S+1L	9.4	Cotton flocks	square	6.6	7.6
-	-	-	Cotton flocks	disc	8.0	2.9
Cab-O-Sil®	S+1L	8.6	Cab-O-Sil®	square	7.2	7.6
-	-	-	Cab-O-Sil®	disc	8.0	2.9
Rhino™ 9700	S+3L	5.6	-	-	-	-
Peel Ply	S+2L	5.5	Peel Ply	square	1.0	7.9
GC 253PA	S+3L	5.0	GC 253PA	disc	7.9	2.9
GC 1 050	S+3L	5.5	GC 1 050	disc	8.0	2.9
Fluorinated Plastic	S+1L	5.4	-	-	-	-
PVC60 Foam	S+1L	10.4	PVC60 Foam	square	5.0	7.2
-	-	-	90070 Glass	square	0.5	8.8
-	-	-	Carbon 98141	square	1.3	7.8
-	-	-	Carbon 9001 MDL	square	1.0	7.1

3.6.3 Manufacturing

Samples were made in batches. Several variants were made per batch and several (four or eight) samples of each variant were made. In total there were 28 variants – 11 permeability and 17 absorption – and 212 samples (3 variants only had 4 samples). All experiment-specific samples were made within 48 hours of each other in similar environmental conditions. The same MGS LR285 epoxy resin and the same MGS LH287 epoxy hardener were used on all fibre-reinforced and filler samples. Fibre orientation of fabrics was 0° (parallel) in all laminate layers of PMCs.

i. Permeability samples

Most permeability sample variants were made during one process while sample variants with paint-on materials (gelcoats and Rhino™ 9700) and fillers had to be manufactured in two phases. The one phase samples were all made by vacuum bagging all components together. Two phase samples were manufactured by first vacuum bagging the substrate components and only applying the filler or coating afterwards.

Due to the non-uniform surface of many samples, a marking was added to each sample (refer to Figure 20) to indicate where the thickness of the sample was to be measured with the micrometer. This assisted in obtaining more consistent readings.

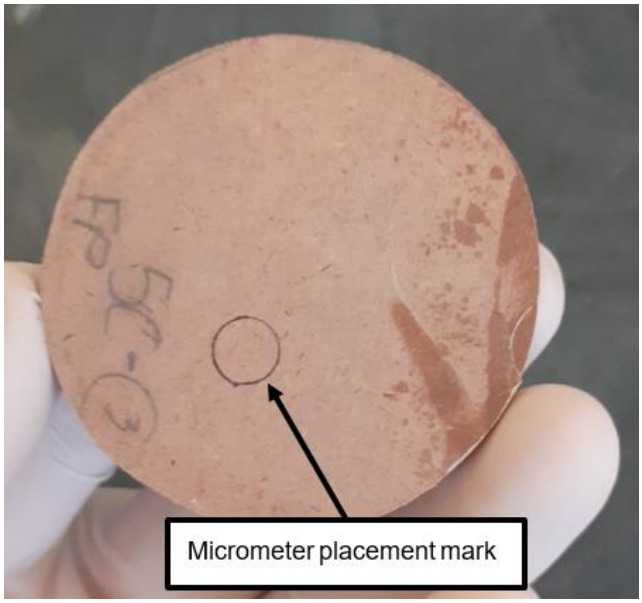

Figure 20: Permeability sample with mark showing where micrometer should be placed when measuring thickness

ii. Absorption samples

PMC absorption samples were also made using the vacuum bagging process. Samples made of coating materials were all casted in PVC pipes, allowed to cure and then cut into discs. Disc-shaped filler samples were made using the same cast and cutting-process as the coating materials, while square shaped samples were merely compressed to the desired thickness before curing and then cut after curing. Control material samples and PVC60 Foam were simply cut into squares from large pieces of off-the-shelf material.

As with the permeability samples, markings were made on the samples (as shown in Figure 21) to assist in measuring a sample's dimensions on the same location each time.

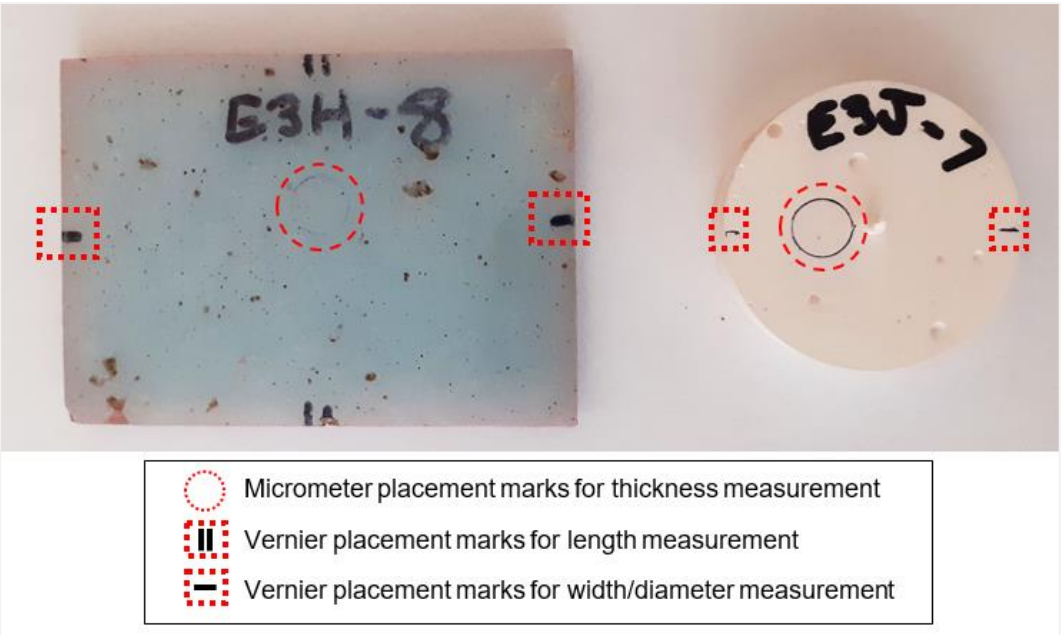

Figure 21: Square and disc samples with measurement marking locations indicated

3.7 Measurement system analysis

The experimental measuring method uncertainty was analysed in terms of dimensional and mass measurements. Uncertainty of measurement is defined by ISO (2004) as a "*parameter that characterizes the dispersion of the quantity values that are being attributed to a measurand*". ISO (2004) goes on to note that measurement uncertainty is comprised of various components. In this specific investigation measurement uncertainty includes factors such as instrument resolution, parallax errors, measurement drift on electronic instruments and operator limitations.

The measuring method and associated instruments were evaluated for approximate uncertainty, represented by the symbol δ in this document. The various measurement uncertainty parameters were determined per variant. Obtaining each variant's variable uncertainty individually meant that any two variants did not necessarily have the same measurement uncertainty for a given parameter. These differences in uncertainty values could be attributed to varying water retention properties (influenced by porosity, surface imperfections, etc.) in the different sample variants. The results of measurement system analysis in the form of uncertainty values are listed in among the results (Section 5.3).

3.7.1 Dimensional measurement analysis

Dimension measurements were analysed by measuring a dry random sample from each of the 28 different variants (including 17 absorption and 11 permeability samples). After recording each sample variant's dimensions, those recordings were hidden to prevent proceeding readings from being influenced by user bias. This process was repeated eight times. The standard deviation was then calculated per variant and used to quantify the measurement uncertainty (refer to Chapter 4.1).

3.7.2 Mass measurement uncertainty

Mass measurement accuracy (MMA) had two main aspects to consider, namely wet and dry sample mass measurement. Dry mass measurement accuracy (DMMA) was mostly effected by sample dryness and scale accuracy (drift, precision, etc.). Wet mass measurement accuracy (WMMA) was effected by the same factors as DMMA, but with the addition of several more significant factors including weighing time, sample saturation and drying effectiveness. These factors shall now be described before explaining the procedure for evaluating DMMA and WMMA. The data from DMMA and WMMA evaluation was then be used to approximate measurement uncertainties, as will be explained in the next section.

Weighing time was taken as the time elapsed from when a sample's direct contact with water source was broken until obtaining a reading on the mass scale. The longer the weighing time, the more sample moisture would be lost to evaporation. This effect was limited by consistently limiting the weighing time to under one minute (as previously specified in the experimental procedures) – typically being closer to 40 than 60 seconds.

The next two factors effecting uncertainty margins of mass readings have to do with sample saturation. There were essentially two saturation types for a sample, namely atmospheric saturation and water saturation. Atmospheric moisture saturation is the level of airborne water vapour which is absorbed by the sample. This only effected permeability samples in a significant way since one side of the samples was always open to the atmosphere. Water saturation, as the name suggests, is merely the level of liquid water that has permeated the sample.

Drying effectiveness is a measure of how effectively water present both on and in the sample is removed with paper towels and/or drying cloth during the weighing time.

This parameter can be expressed as a percentage. Ideal drying effectiveness could theoretically be achieved by removing all surface water on the sample without over-drying the sample. Over-drying occurs when water that was absorbed by the sample, is extracted when wiping or patting the sample dry with a paper towel/drying cloth.

DMMA was done primarily as a form of control experiment for permeability testing. DMMA was carried out with absorption samples as well to independently (with no substrate) quantify the different materials' proclivity to absorb moisture from the atmosphere. DMMA evaluation was done on samples on the same day they were removed from the oven after drying. A sample from each variant of both permeability and absorption categories was randomly selected and weighed on the scale (both scales listed in Table 2 in Section 3.2 were tested). These electronically recorded readings were then temporarily hidden from sight before measuring each of the selected samples again. This process of measure, record and hide recording was repeated nine times.

WMMA was quantified by taking samples at peak atmospheric saturation. Peak atmospheric saturation was conservatively taken to be reached comfortably by a thousand hours of exposure to only open air (not in sealed containers). Samples were randomly selected in the same way as with DMMA evaluation. WMMA evaluation started with one dry reading of each sample. The recordings were then temporarily hidden from view. Each sample would then be exposed to liquid water for 3-5 seconds – only on the area(s) that would be exposed in normal testing specified in Section 3.3 and 3.4. Within the next 40-50 seconds the sample had to be dried with a paper towel and/or cloth, placed on the scale and the mass recorded. The exposure period was dictated to be so short in order to allow minimal time for absorption of liquid water to take place, which would then leave only significant amounts of surface water to be dried. If the drying method was efficient, this second mass reading would be nearly the same as the first, with the WMMA being of similar magnitude to DMMA. The WMMA analysis did not include any more sets of readings beyond the second set, since repeated exposure lead to an increased build-up of imbedded moisture that could not be extracted by using paper towels or drying cloth, leading to unrealistically large deviation from the first mass recorded.

3.8 Summary

This chapter described the means by which experimental data was acquired and the steps taken in preparation for conducting the investigation. The setup and procedure of

absorption and permeability experiments were explained. Furthermore, the samples along with their material properties and manufacturing details were discussed. The method for evaluating accuracy of the experimental method was also specified in terms of the measurement system analysis.

4 Data Processing

Execution of the experimental method of both absorption and permeability testing would yield hundreds of data entries per test. It was reasonable to expect that not all data would accurately represent a material's characteristics due to factors not pertaining to the material itself, but rather to the method. Even among the acceptable data, processing methods had to be implemented to ascertain the accuracy of values reported. The subsequent sections explain the methods used to quantify uncertainty, remove outliers, select representative data, and finally process results into a comparable format.

4.1 Measurement uncertainty and error propagation

The MSA described in Section 3.7 provided a series of measurements per measurable variable of each sample variant. Each series of measurements could then be used to determine the approximate uncertainty (δ) associated with each sample variants' measured variables ($MV\#$). The measured variables were sample dimensions and mass. The measurement uncertainty was taken to be

$$\delta_{MV\ \#,Var\ \#} = 2\sigma_{MV\ \#,Var\ \#}$$

with σ being the standard deviation of the readings of a particular sample variant ($Var\ \#$). This provides a 95.4% probability that a measurement will lie within 2σ of the actual value (Taylor, 1997). In order to incorporate the measurement uncertainties in subsequently calculated values, effects of error propagation or cumulative error were accounted for.

4.2 Removal of outliers and percentile value selection

Since multiple samples of each variant were made, there were inter-variant differences in readings among samples. It also meant that some samples would potentially display outlier behaviour due to variances in sample composition or measurement uncertainty. Then once outliers had been removed, then a conservatively high representative value would be taken – namely a 95th percentile value. The following process was followed to remove outliers and obtain 95th percentile values:

a) Recordings from permeability sample testing rigs that had visible leaks at the o-ring were not included in further processing (refer to Figure 22 and Figure 23). Leaks were not an issue with absorption samples, as they were totally immersed.
b) Less obvious outliers were defined as those outside the range

$$M \in [Q1 - 1.5 \times IQR; Q3 + 1.5 \times IQR]$$

where Q is the quartile (inclusive) and IQR is the interquartile range. If a sample had one outlier reading, all the readings of that sample for the associated round of testing were disregarded in further processing. The IQR was not recalculated after removal of outliers.

c) Manual identification of outliers was done in instances where multiple outliers of a variant in a round increased the 1.5 IQR to the point that it was still allowing recordings that appeared to be outliers.

d) The 95th percentile of each variant across the four rounds of testing was then used to determine mass gain and moisture content. The 95th percentile was chosen as this returned conservative (high) representative values of moisture gain from each variant. This provided a value demonstrative of a worst-case scenario in terms of a material's resistance to absorption and water permeability.

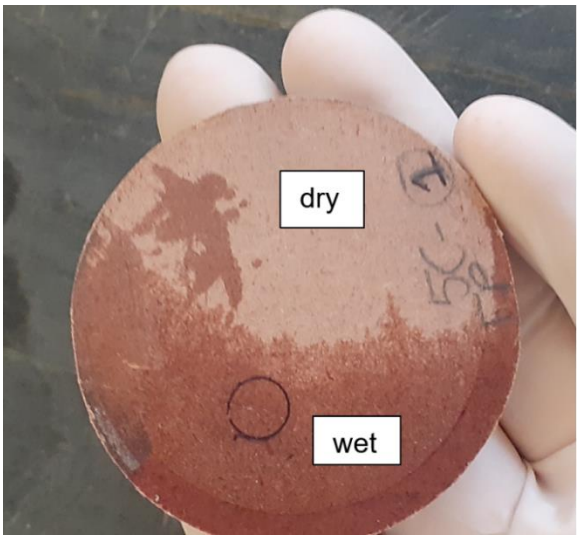

Figure 22: Partly wet underside of a fluorinated plastic sample that leaked on one side

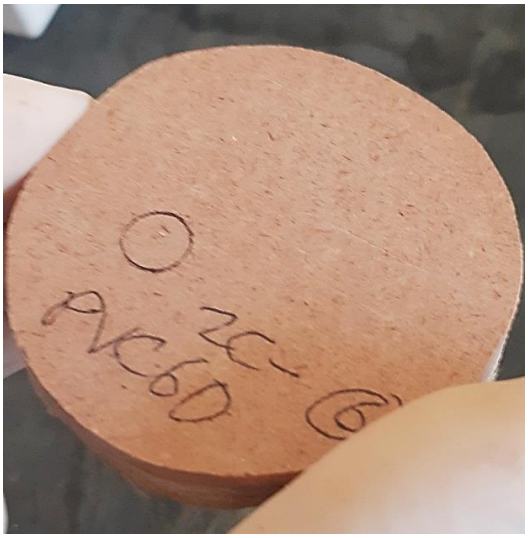

Figure 23: Totally dry underside of a PVC60 sample

4.3 Scoring criteria

In some instances, certain sample variables made direct comparison of moisture content and mass gain inaccurate. Consequently, a sequence of scoring criteria was established to normalize the results. Unique scoring criteria for each of the two experiment types was established as will be described below and are summarised in Table 5.

4.3.1 Permeability criteria

Permeability is a function of the several factors including layer thickness (Newill *et al.*, 1999) as well as material properties such as density, free volume, hygroscopic swelling, capillarity (Choudalakis & Gotsis, 2012b; Manujesh *et al.*, 2014; Maxwell *et al.*, 2005; Shirangi & Michel, 2010). Due to the highly contrasting material properties of the components (test material, Glass 92125 and MDF) found in permeability samples, they contributed in different proportions to the observed mass increase. This implies that the measured moisture content measured in a permeability sample variant ($M_{[P],Variant\ \#}$) is the sum of the moisture absorbed by each component.

$$M_{[P],Variant\ \#} = (M_w + M_d)_{S,\#} + (M_w + M_d)_{ct,\#} \quad \text{(Eq 4)}$$

where $(M_w + M_d)_{S,\#}$ is the moisture gain percentage of a substrate of the specified variant. $(M_w + M_d)_{ct,\#}$ is the moisture gain percentage of the coating of that variant. M_w and M_d correspondingly represent moisture gain percentage in wet and dry sub-variations of the permeability experiment (procedure as explained in Section 3.3). The meanings of the different subscripts are listed in NOMENCLATURE AND SYMBOLS.

The substrate of all non-control samples – although similar – was not identical when comparing different variants. Also, due to the physical consistency of coatings (some being less viscous and more fluid than others), coating layers were not of identical mass or thickness. Refer to Figure 24 for a diagram showing how the thicknesses differed. Some samples' top layers consisted of fabrics/materials of specific thickness which differed from those of other sample variants. These factors all mean that when comparing any two sample variants' moisture contents (for demonstration purposes, the placeholder "#" will be replaced with material 1 and 2 to represent different sample variants) and it be found that

$$M_{[P],Variant\ 1} < M_{[P],Variant\ 2} \quad \text{(Eq 5)}$$

It cannot be implied with certainty that

$$(M_w + M_d)_{ct,1} < (M_w + M_d)_{ct,2} \quad \text{(Eq 6)}$$

because there's a great possibility that

$$(M_w + M_d)_{S,1} \neq (M_w + M_d)_{S,2} \quad \text{(Eq 7)}$$

Another complication in the observed moisture content is that some of the moisture that was absorbed by the substrate came from airborne moisture in the atmosphere and did not permeate through the test material component.

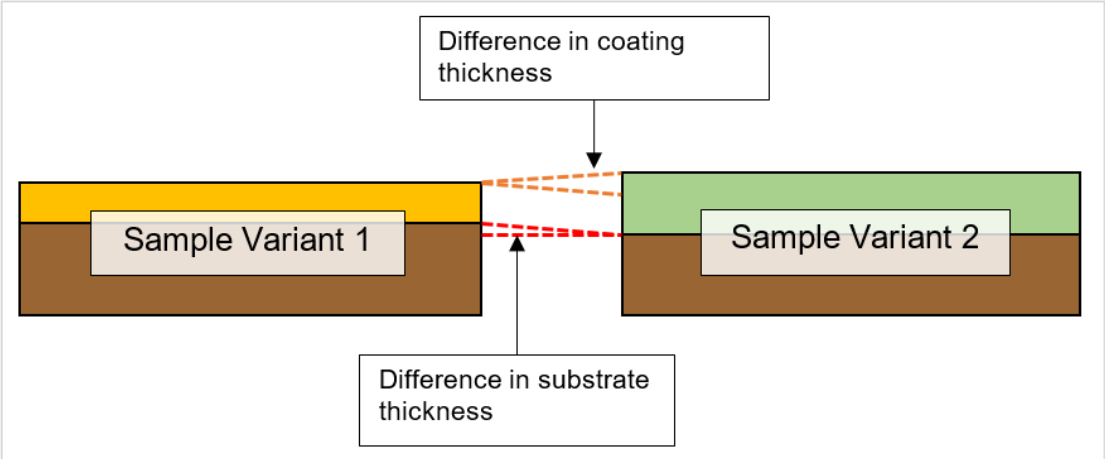

Figure 24: Diagram showing two ways in which permeability sample variants can differ – making direct comparison of coating material characteristics more intricate.

Two groups of criteria were constructed to address this insufficiency in permeability data. These criteria were used to determine a permeability rank-score.

i. Dry versus wet performance

The catchment seal of the permeability rig was not airtight, so atmospheric moisture outside the rig could be absorbed by the sample. As depicted in Figure 25, atmospheric moisture could also reach the sample from above in the dry experiment, since there was no liquid water barrier to diffuse through. It is also easier for water vapour molecules to permeate through materials than it is for liquid water molecules. Thus, it was expected that if the test material component (the top component of the sample) provided very low liquid water permeability, the sample would absorb **less** moisture during the wet experiment than during the dry version of the experiment. Inversely, if the sample had high liquid water permeability, it would absorb **more** during the wet experiment than the dry version of the experiment. A parameter (β) was used to compare the wet-to-dry moisture content ratio of different variants. The wet-to-dry moisture content ratio at a specific time (β_t) was defined as

$$\beta_t = \left(\frac{M_w}{M_d}\right)_{t,Variant:[P]} \quad \text{(Eq 8)}$$

Permeability is directly proportional to the magnitude of β. The effect of varying substrate thicknesses and masses was negated since substrates of the same variant were very similar.

β-values were then used to determine a β-score. Test materials were then ranked according to their β-values in descending order from $N_{[P]}$, the number of permeability sample variants, to one. Materials with lower β-values obtained higher β-Scores. The β-Score was used as a primary indicator of a test material's permeability, since it was one of the most objective values for comparison purposes.

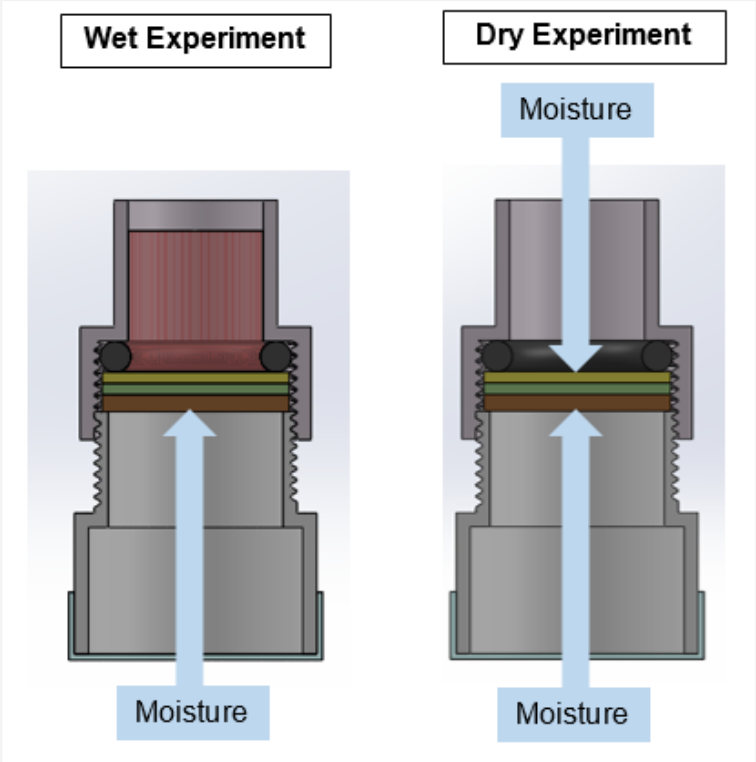

Figure 25: Paths by which atmospheric moisture reaches the sample in the wet and dry experiment formats

ii. Sample mass gain relative to substrate

By making use of the wet and dry experiment data obtained from testing the substrate-only control (92125 Glass – 6L) samples, a deduction could be made with regards to the relative performance of a test material whilst taking the differing substrate compositions of the variants into consideration. The variable $\propto$ was chosen to represent the ratio of dry (d) mass gain of a specific sample variant ($\Delta m_{\text{Variant: [P]}}$) to the dry mass gain of the substrate-only variant ($\Delta m_{92125\ \text{Glass: [P]}-\ 6L}$) at a specific time ($t$). The α-value was associated with dry experimental data and was formulated as

$$\propto_{t,d,[P]} = \left(\frac{\Delta \text{m}_{\text{Variant: [P]}}}{\Delta \text{m}_{92125\ \text{Glass: [P]}-\ 6L}}\right)_{t,d} \qquad \text{(Eq 9)}$$

Similarly, another variable (γ) denoted the ratio of wet (w) mass gain of a specific sample variant to the wet mass gain of the substrate-only variant at a specific time. The γ-value was mathematically expressed as

$$\gamma_{t,w,[P]} = \left(\frac{\Delta m_{Variant:\,[P]}}{\Delta m_{92125\ Glass:\,[P]-\,6L}}\right)_{t,w} \qquad \text{(Eq 10)}$$

If the α-value was larger than 1, it would imply that in dry conditions the test material sample absorbed more moisture than the substrate-only control sample which, in turn, was indicative of

- a larger and/or more absorbent substrate in the test sample variant, AND/OR
- a more absorbent test material or a test material on which a larger amount of surface moisture could accumulate (due to surface pores which effectively increase the exposed surface area).

If the γ-value was larger than 1, the test material sample absorbed more moisture than the substrate-only sample. However, this could be due to more absorbent characteristics of the substrate of the test sample – not necessarily the test material itself. Only if the α-value was less than one **and** the γ-value was larger than one, could the verdict be made that the test material had high permeability. The opposite held true if the α-value was more than one **and** the γ-value was less than one. The drawback of this deduction is that it is not conclusive in the two remaining scenarios. Because several test samples would receive no verdict on this criterion, it was decided that the contribution of this criterion in the form of the αγ-Score would be one, zero, or minus one – depending on the combination of α and γ-values (refer to Table 5). It would become biased if certain materials' permeability rating were heavily influenced (i.e. with larger value scores) by αγ-Score while certain materials were only allocated a zero. Since the outcome of a "no-verdict" scenario is neutral, it neither benefits nor detracts from the permeability rating of the material.

In order to combine the β and αγ-Scores, a permeability rank-score ($\Pi_{[P]}$) was formulated to provide a numerical score above 0 and up to a maximum of 10. The variable Π denotes a weighted summation of scores obtained from the criteria variables previously described. The higher the $\Pi_{[P]}$-value, the higher the permeability. The permeability rank-score was defined in the following general format:

$$\Pi_{[P],Variant\ \#} = \left(\mathrm{A}_{[P]}\right)[\mathrm{C}_{[P]} - (\mathrm{D}_{[p]} \cdot \beta\text{-}Score_{Variant\ \#} + \alpha\gamma\text{-}Score_{Variant\ \#})]$$

$$where\ \mathrm{A}_{[P]}, \mathrm{C}_{[P]}\ and\ \mathrm{D}_{[P]}\ are\ positive\ permeability\ constants$$
$$\{\Pi_{[P]} \in \mathbb{Q} | 0 < \Pi_{[P]} \leq 10\}$$
$$\{\beta\text{-}Score \in \mathbb{Z} | 1 \leq \beta\text{-}Score \leq N_{[P]}\}$$
$$\{\alpha\gamma\text{-}Score \in \mathbb{Z}\} = \{-1,0,1\} \quad \text{(Eq 11)}$$

$\mathrm{D}_{[P]}$ was arbitrarily chosen to be 2 so that the sum of $\beta\text{-}Score$ and $\alpha\gamma\text{-}Score$ would not be negative. The constant A served as a divisor or fraction to ensure that the maximum permeability score would be 10 (arbitrarily selected as a common maximum for both permeability and absorption rank-scores).

By setting up conditions under which maximum and minimum permeability scores would be achieved the constants could be determined as follows:

$$Let\ Y_{[P]} = (\mathrm{D}_{[P]} \cdot \beta\text{-}Score\ + \alpha\gamma\text{-}Score)$$
$$= 2\beta\text{-}Score\ + \alpha\gamma\text{-}Score \quad \text{(Eq 12)}$$

and

$$Let\ Q_{[P]} = [\mathrm{C} - (2\beta\text{-}Score\ + \alpha\gamma\text{-}Score)]$$
$$= \mathrm{C} - Y \quad \text{(Eq 13)}$$

so that

$$\Pi_{[P],MAX} = \left(\mathrm{A}_{[P]}\right)[\mathrm{C}_{[P]} - Y_{[P],MIN}]$$
$$10 = \left(\mathrm{A}_{[P]}\right)[\mathrm{C}_{[P]} - Y_{[P],MIN}]$$
$$\mathrm{A}_{[P]} = \frac{10}{\mathrm{C}_{[P]} - Y_{[P],MIN}} \quad \text{(Eq 14)}$$

and

$$P_{MIN} = \mathrm{C} - Y_{MAX}$$
$$1 = \mathrm{C} - Y_{MAX}$$
$$C = 1 + Y_{MAX} \quad \text{(Eq 15)}$$

Then substitute (Eq 15) into (Eq 14) to solve for $\mathrm{A}_{[P]}$

$$\mathrm{A}_{[P]} = \frac{10}{(1 + Y_{[P],MAX}) - Y_{[P],MIN}} \quad \text{(Eq 16)}$$

Take note that Y_{MIN} is the lowest total of $\beta\text{-}Score$ and $\alpha\gamma\text{-}Score$ to be attributed to a specific material. Although the lowest possible value of Y_{MIN} is one, the lowest actual sum in this specific study of the β and $\alpha\gamma\text{-}Scores$ had the potential to be greater than one if the $\alpha\gamma\text{-}Score$ of a variant was zero or one (instead of minus one). The same principle holds for Y_{MAX} – which consequently influences the value of C. Although, any number would have sufficed, a value of one was attributed to P_{MIN} in order to solve for A and C. Finally, (Eq 11) can be rewritten as

$$\Pi_{[P],Variant\ \#} = \left(\frac{10}{1 + Y_{[P],MAX} - Y_{[P],MIN}}\right)[1 + Y_{[P],MAX} - Y_{[P],Variant\ \#}] \quad \text{(Eq 17)}$$

4.3.2 Absorption criteria

i. Moisture content

Due to absorption samples' homogenous composition, the moisture content percentage (as described in Section 2. LITERATURE REVIEW) at a specific time in wet testing could be used for assessing a material's relative performance. Higher moisture content percentage simply indicates higher absorption rate and/or capacity. Higher moisture content led to a lower $M\text{-}Score$. The $M\text{-}Score$ is a measure of how resistant the material is to water absorption.

ii. Mass gain per unit exposed area

The differing sizes of sample variants caused significant differences in mass gain. This effect was normalized by using a ratio. The mass gain during wet testing, Δm_w, per unit exposed area, A_{exp}, was calculated with the following ratio

$$\theta_{w,t} = \left(\frac{\Delta m_w}{A_{exp}}\right)_{t,Variant\ \#:\ [A]} \quad \text{(Eq 18)}$$

Higher θ-value led to a lower $\theta\text{-}Score$, since the $\theta\text{-}Score$ is a rating of how resistant the material is to water absorption in relation to its exposed area.

These criteria scores are used to determine the absorption rank-score ($\Pi_{[A]}$). The sample variant's absorption is directly proportional to the $\Pi_{[A]}$-value. Similar to how the permeability rank-score was formulated, the absorption rank-score with its unknowns was defined as

$$\Pi_{[A],Variant\,\#} = (A)[\mathrm{C} - (M\text{-}Score_{Variant\,\#} + \theta\text{-}Score_{Variant\,\#})]$$

$$where\ \mathrm{A}_{[A]}, \mathrm{C}_{[A]}\ and\ \mathrm{D}_{[A]}\ are\ positive\ absorption\ constants$$
$$\{\Pi_{[A]} \in \mathbb{Q} \mid 0 < \Pi_{[A]} \leq 10\}$$
$$\{M\text{-}Score \in \mathbb{Z} \mid 1 \leq M\text{-}Score \leq N_{[A]}\}$$
$$\{\theta\text{-}Score \in \mathbb{Z} \mid 1 \leq \theta\text{-}Score \leq N_{[A]}\}$$
$$with\ N_{[A]} = \ the\ number\ of\ absorption\ sample\ variants \qquad \text{(Eq 19)}$$

There is no D constant required in (Eq 19) because the sum of the $M\text{-}Score$ and the $\theta\text{-}Score$ is, by the constraints of the variables, always positive. Additionally, these two scores are equally important in assessing absorption performance, so they receive the same default weighting (i.e. one). In the same manner as with the permeability rank-score equation, the constants were solved by doing similar substitutions as shown in (Eq 20) and (Eq 21).

$$Let\ Y_{[A]} = (M\text{-}Score\ + \theta\text{-}Score) \qquad \text{(Eq 20)}$$

and

$$Let\ Q_{[A]} = [\mathrm{C}_{[A]} - (M\text{-}Score\ + \theta\text{-}Score)] = \mathrm{C}_{[A]} - Y_{[A]} \qquad \text{(Eq 21)}$$

Finally, the absorption rank score of a sample variant is

$$\Pi_{[A],Variant\,\#} = \left(\frac{10}{1 + Y_{[A],MAX} - Y_{[A],MIN}}\right)\left[1 + Y_{[A],MAX} - Y_{[A],Variant\,\#}\right] \qquad \text{(Eq 22)}$$

Table 5: List of criteria and associated details for scoring the materials tested

No.	Parameters	Outcomes
1	β_t	$If \begin{Bmatrix} \beta_t > 1 \rightarrow high\ permeability; low\ \beta\text{– score} \\ \beta_t < 1 \rightarrow low\ permeability;\ high\ \beta\text{– score} \end{Bmatrix}$
2	$\propto_{t,d,[P]}$ $\gamma_{t,w,[P]}$	$If \begin{Bmatrix} \propto_{t,[P]} > 1 \text{ and } \gamma_{t,w,[P]} < 1 \\ \rightarrow low\ water\ permeability\ of\ coating;\ \alpha\gamma\text{-}Score = 1 \\ \propto_{t,[P]} < 1 \text{ and } \gamma_{t,w,[P]} < 1 \rightarrow no\ verdict;\ \alpha\gamma\text{-}Score = 0 \\ \propto_{t,[P]} > 1 \text{ and } \gamma_{t,w,[P]} > 1 \rightarrow no\ verdict;\ \alpha\gamma\text{-}Score = 0 \\ \propto_{t,[P]} < 1 \text{ and } \gamma_{t,w,[P]} > 1 \\ \rightarrow high\ water\ permeability\ of\ coating;\ \alpha\gamma\text{-}Score = -1 \end{Bmatrix}$
3	$M_{w,t,[A]}$	$Lower\ \ M_{w,t,[A]} \rightarrow Lower\ moisture\ absorption; higher\ M\text{-}Score$ $Higher\ \ M_{w,t,[A]} \rightarrow Higher\ moisture\ absorption; lower\ M\text{-}Score$
4	$\theta_{w,t}$	$Lower\ \theta_{w,t} \rightarrow Lower\ moisture\ absorption; higher\ \theta\text{-}Score$ $Higher\ \theta_{w,t} \rightarrow Higher\ moisture\ absorption; lower\ \theta\text{-}Score$

4.4 Summary

The procedure of a novel approach to quantify permeability by means of measuring the moisture increase in a substrate underneath the test material was specified along with an adaptation of the more common gravimetric water absorption testing procedure.

The methods and techniques used to process measured data were also discussed. The unique scoring criteria which would help normalize the effects of dissimilar permeability substrates and differing absorption sample sizes was also described.

5 RESULTS

The fully processed data are analysed in this chapter. Firstly, absorption and permeability results of each variant are given in the basic form of moisture content and mass gain. Next, the resulting rank score implementation is explained before going on to compare and discuss material performance by material category. Finally, validation and verification of results are addressed.

5.1 Moisture content and mass gain results

The initial mass as well as the mass gain and moisture content at 300 hours (for both wet and dry tests) are listed in Table 6 and

Table 7. It can be noted from the M-values in both permeability and absorption experiments that MDF had the highest moisture content by a large margin.

It can also be pointed out that polypropylene control samples did not exhibit the lowest permeability moisture content ($M_{[P],w,300h}$) as expected in relation to other coating materials, despite displaying the lowest moisture content ($M_{[A],w,300h}$) of all tested materials during absorption experimentation. This further reinforces the necessity for additional criteria as explained in Section 4.3.

Table 6: Initial mass, mass gain and moisture content of all permeability sample variants

		Wet		Dry	
Material & Variant	**m_0[2] [g]**	**$\Delta m_{w,300h}$ [g]**	**$M_{w,300h}$ [%]**	**$\Delta m_{d,300h}$ [g]**	**$M_{d,300h}$ [%]**
92125 Glass: [P]	14.57	0.52	3.58%	0.345	2.37%
Cab-o-Sil: [P]	25.14	0.15	0.61%	0.158	0.63%
Cotton flocks mix: [P]	26.78	0.47	1.77%	0.477	1.78%
Fluorinated plastic: [P]	15.96	0.57	3.56%	0.335	2.10%
GC 1050: [P]	17.12	0.29	1.72%	0.392	2.29%
GC 253PA: [P]	15.16	0.31	2.03%	0.409	2.70%
Gurit PVC60 Foam 5mm: [P]	17.26	0.37	2.12%	0.381	2.21%

[2] m_0 is an average value and not a 95th percentile value

		Wet		Dry	
Material & Variant	**m_0[2] [g]**	**$\Delta m_{w,300h}$ [g]**	**$M_{w,300h}$ [%]**	**$\Delta m_{d,300h}$ [g]**	**$M_{d,300h}$ [%]**
Peel ply: [P] - 2L	15.46	0.56	3.63%	0.353	2.28%
Polypropylene: [P]	16.19	0.28	1.72%	0.418	2.58%
Rhino 9700: [P]	16.85	0.54	3.210%	0.431	2.56%
MDF: [P]	5.83	10.62	182.2%	1.119	19.2%

Table 7: Initial mass, mass gain and moisture content of all absorption sample variants

		Wet		Dry	
Material & Variant	**m_0 [g]**	**$\Delta m_{w,300h}$ [g]**	**$M_{w,300h}$ [%]**	**$\Delta m_{d,300h}$ [g]**	**$M_{d,300h}$ [%]**
9001 MDL Carbon: [A] - 6L	4.18	0.07	1.67%	0.026	0.63%
90070 Glass: [A] - 6L	2.93	0.14	4.88%	0.019	0.64%
92125 Glass: [A] – 4 mm plate	29.18	0.10	0.33%	0.038	0.13%
92125 Glass: [A] - 6L	7.95	0.14	1.82%	0.043	0.54%
92125 Glass: [A] – 6 mm plate	40.51	0.11	0.27%	0.053	0.13%
98141 Carbon: [A] - 6L	5.96	0.10	1.70%	0.035	0.59%
Cab-o-Sil: [A] – disc	8.69	0.08	0.94%	0.042	0.48%
Cab-o-Sil: [A] – square	24.22	0.18	0.76%	0.082	0.34%
Cotton flocks mix: [A] – disc	8.91	0.13	1.43%	0.059	0.66%
Cotton flocks mix: [A] - square	23.11	0.33	1.43%	0.127	0.55%
GC 1050: [A] – disc	12.38	0.04	0.29%	0.019	0.15%
GC 253PA: [A] – disc	10.94	0.03	0.28%	0.021	0.19%
Gurit PVC60 Foam 5mm: [A]	0.91	0.37	40.72%	0.004	0.40%
Peel ply: [A] - 6L	3.12	0.34	10.9%	0.115	3.68%
Polypropylene: [A]	2.97	0.01	0.21%	0.001	0.03%
Rhino 9700: [A] – disc	9.52	0.05	0.50%	0.024	0.25%
MDF: [A]	7.67	12.26	160%	1.02	13.3%

5.2 Implementation of rank-score Equations

Experimental data was used to determine the numerical values the unknown constants associated with permeability and absorption rank-score equations described in the previous chapter. The values of these variables are listed in Table 8.

Table 8: Experimental variable values

Variable	Value
$Y_{[P],MAX}$	23
$Y_{[P],MIN}$	2
$N_{[P]}$	11
$Y_{[A],MAX}$	34
$Y_{[A],MIN}$	2
$N_{[A]}$	17

Substitution of these numerical values into equation (Eq 17) meant that the permeability rank-score became

$$\Pi_{[P],Variant\ \#} = \left(\frac{10}{1+(23)-(2)}\right)\left[1+(23)-Y_{[P],Variant\ \#}\right]$$

$$\Pi_{[P],Variant\ \#} = \left(\frac{10}{22}\right)\left[24-Y_{[P],Variant\ \#}\right] \qquad \text{(Eq 23)}$$

$$\Pi_{[P],Variant\ \#} = \left(\frac{5}{11}\right)\left[24-Y_{[P],Variant\ \#}\right]$$

By the same means, the corresponding variables of the absorption rank-score equation (Eq 22) could be substituted and simplified as follows:

$$\Pi_{[A],Variant\ \#} = \left(\frac{10}{1+(34)-(2)}\right)\left[1+(34)-Y_{[A],Variant\ \#}\right]$$

$$\Pi_{[A],Variant\ \#} = \left(\frac{10}{33}\right)\left[35-Y_{[A],Variant\ \#}\right] \qquad \text{(Eq 24)}$$

Figure 26 lists the permeability and absorption rank-scores accumulated in bar graph based on the criteria parameters defined. In this graph it can be seen that polypropylene does offer the best absorption and water permeability resistance if this more holistic approach of rank-scoring is taken. On the other side of the spectrum is the other control material, MDF, which has higher absorptivity and permeability than all the other materials. In order to better assess the relative performance of materials, the results from the scoring criteria will be discussed by category: fillers and coatings, PMC's and foam.

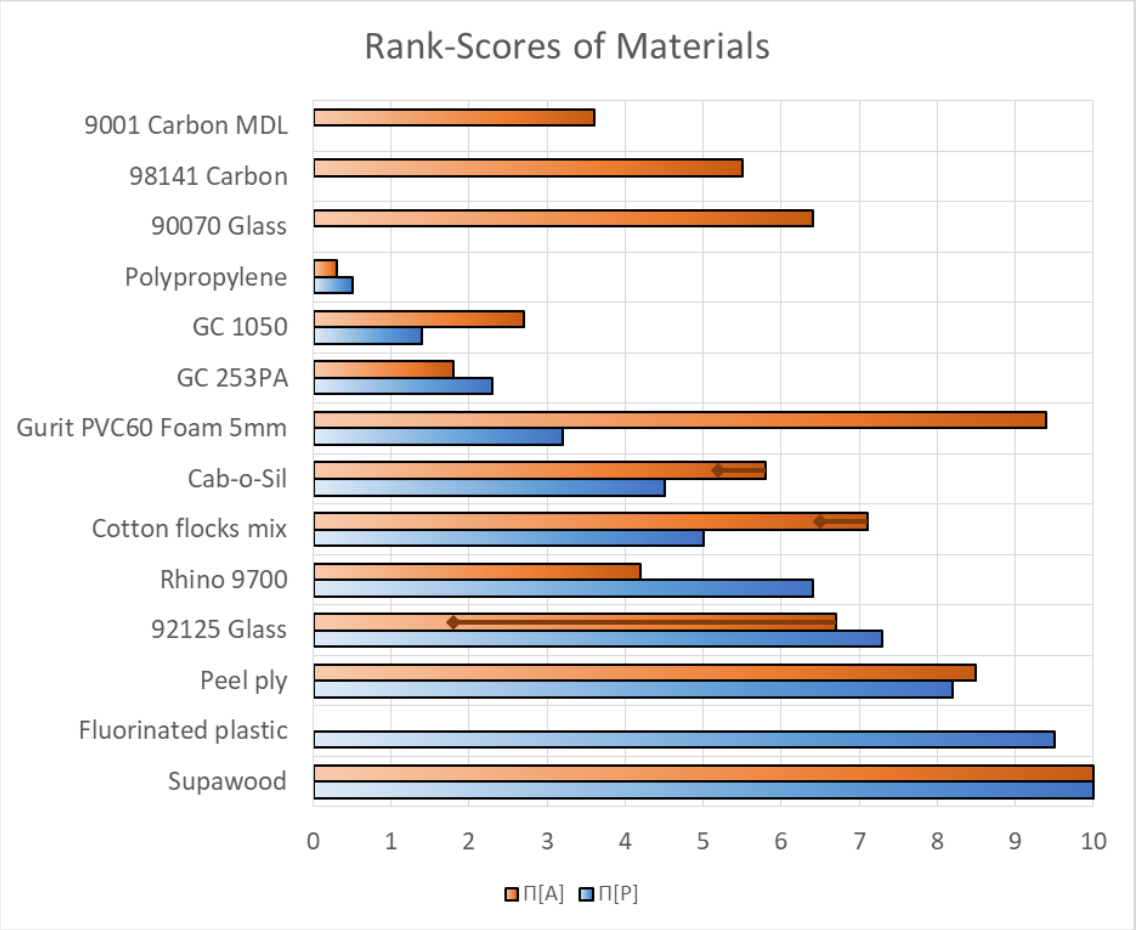

Figure 26: Rank-scores of all materials tested

5.3 Measurement uncertainty and discarded data

This subsection will look at the measurement uncertainty and its propagated effects. Two data processing factors with regards to the results that were discarded are also addressed.

5.3.1 Measurement errors and cumulative effects

Comparison of the magnitudes of mass uncertainties (δm**)**, shows that DMMA (refer to Section 3.7.2 for description) was higher than WMMA in most (13 out of 17) instances. Table 9 below illustrates this point with the uncertainties of absorption sample measurements. As specified in the MSA data processing in Section 4.1 , these mass uncertainties were determined using the standard deviation (σ_m) of the MSA mass readings obtained for each sample variant. This was done with both WMMA and DMMA. Refer to Appendix A for an example calculation of Rhino absorption samples' measurement errors. Recall that there were only **two** WMMA readings per variant as while **nine** readings were taken per variant sample with DMMA (refer back to Section 3.7.2 for explanation).

Dry measurements tended to have lower uncertainty than the wet measurements of the same material. This higher inaccuracy in wet mass measurement can be ascribed to the added variable of fluctuating drying effectiveness. Drying effectiveness depended on several factors which could not be controlled well. These factors include sample texture, sample hardness, drying towel's dryness, force applied by hand when drying or wiping the sample.

Table 9: Absorption testing mass measurement uncertainty (dry and wet)

Material	δm_{DMMA} [g]	δm_{WMMA} [g]
9001 Carbon MDL	0.0002	0.0042
90070 Glass	0.0005	**0.0003**
92125 Glass	0.0003	0.0023
98141 Carbon	0.0002	0.0004
Gurit PVC60 (just foam)	0.0003	0.0206
Cab-o-Sil filler (casted)	0.0003	0.0028
Cab-o-Sil filler (compressed)	0.0005	0.0104
Control - Just wood	0.0057	0.1047
Control - PP Plastic	0.0002	0.0006
Cotton flocks mix (casted)	0.0003	0.0011
Cotton flocks mix (compressed)	0.0004	**0.0002**
GC 1050	0.0020	**0.0003**
GC 253PA	0.0002	0.0002
Glass 92125 – 4 mm plate	0.0004	0.0043
Glass 92125 – 6 mm plate	0.0002	0.0013
Rhino (casted)	0.0003	**0.0001**
Peelply (6L)	0.0006	0.0176

Table 10 lists the cumulative error on the moisture content of permeability samples after 300 hours. Similarly, Table 11 gives the cumulative error of absorption samples. The variants are sorted in order of ascending relative error. The relative error or fractional uncertainty ($\delta M/M$) in both experiment types is shown to never exceed the generally acceptable uncertainty of 5%. Where a range is given, it is because multiple sub-variants of the same material was made and had differing values of which the maximum and minimum are displayed.

Generally, a lower level of accuracy was found in measurement of absorption samples, probably because effectively drying a sample that was totally submerged was much harder than drying a sample that was only wet on one surface. Absorption testing still had a maximum fractional uncertainty that reached merely 2%.

The moisture content values in Table 10 and Table 11 were rounded up to either two decimal places or for values larger than 1%, up to three significant figures. The error (δM) values were rounded to the same number of significant figures as the moisture content value. The relative or fractional uncertainty ($\delta M/M$) was shown accurate to

one significant figure. Refer to Section 5.6.1 for an example of how the cumulative error was determined using the guidelines provided in Section 2.4.

Table 10: Moisture content after 300 hours and cumulative uncertainty associated with wet mass measurement of permeability sample variants

Material	$M_{wet,300h,[P]}$ [%]	$\delta_{M,300h,[P]}$ [%]	δM/M [%]
Cab-o-Sil	0.61%	0.00%	0.01%
Cotton flocks mix	1.77%	0.00%	0.01%
GC 1050	1.72%	0.00%	0.02%
GC 253PA	2.03%	0.00%	0.02%
Fluorinated plastic	3.56%	0.00%	0.02%
Rhino 9700	3.21%	0.00%	0.02%
Gurit PVC60 Foam 5mm	2.12%	0.00%	0.03%
Polypropylene	1.72%	0.00%	0.03%
Peel ply	3.63%	0.00%	0.03%
92125 Glass	3.58%	0.00%	0.04%
MDF	182%	5%	3%

Table 11: Moisture content after 300 hours and cumulative uncertainty associated with wet mass measurement of absorption sample variants

Material	$M_{wet,300h,[A[}$ [%]	$\delta_{M,300h,[A]}$ [%]	δM/M [%]
Cotton flocks mix	1.43%	0.00%	0.006-0.02%
GC 253PA	0.28%	0.00%	0.007%
92125 Glass	0.27-1.82%	0.00%	0.008-0.03%
Rhino/Jeffco 9700	0.50%	0.00%	0.009%
98141 Carbon	1.70%	0.00%	0.01%
GC 1050	0.29%	0.00%	0.02%
90070 Glass	4.88%	0.00%	0.02%
Polypropylene	0.21%	0.00%	0.03%
Cab-o-Sil	0.76-0.94%	0.00%	0.04%
9001 Carbon MDL	1.67%	0.00%	0.1%
Peel ply	10.92%	0.1%	0.6%
MDF	159.81%	1%	0.7%
Gurit PVC60 Foam 5mm	40.72%	0.7%	2%

5.3.2 Mass readings with low-resolution scale

Some data had to be discarded over and above that which was detected by the outlier removal criteria specified in Section 4.2. This was because of a significant loss in accuracy in early readings that had to be avoided in further processing.

As mentioned in the experimental setup (Section 3.2), a scale with a resolution of 0.1mg was used for mass measurement. However, for the latter part of Round 1, a low-resolution scale had to be used due to limiting circumstances. This alternative mass scale only had a resolution of 50mg. The result was that measurement uncertainty became excessively large – greater than 10% of the associated value in many instances. In order to retain higher certainty on values reported, measurements obtained with this less-accurate scale were not used during calculations of criteria parameters. These readings with high measurement uncertainty in Round 1 served the purpose of measuring how close to saturation point samples came by 700 to 800 hours. Refer to Figure 27 and Figure 28 for examples of how large the measurement uncertainty became due to the low accuracy mass measurement. Figure 27 shows a large margin of uncertainty in values from 140 hours onwards in Round 1 of permeability testing while Figure 28 illustrates a large margin of uncertainty in values from 170 hours onwards in Round 1 of absorption testing.

Also take note that the error bars of all other data points from subsequent rounds are invisible due to their uncertainty being in the order of 500 times lower. Despite their high degree of uncertainty, these affected values in Round 1 still compare well with higher accuracy values from other rounds. The first round of testing was ultimately discarded so as not to increase the uncertainty in final results reported. The error margins of subsequent rounds were very small and often negligible, as is shown by the nearly insignificant error bars in the graphs of Figure 29, Figure 30 and Figure 31 which represent the cumulative error on moisture content of the various materials. Having a smaller error meant that the possible overlap of values was much more limited, which, in turn, lead to a more definitive distinguishing between the various materials' absorption and permeability performance.

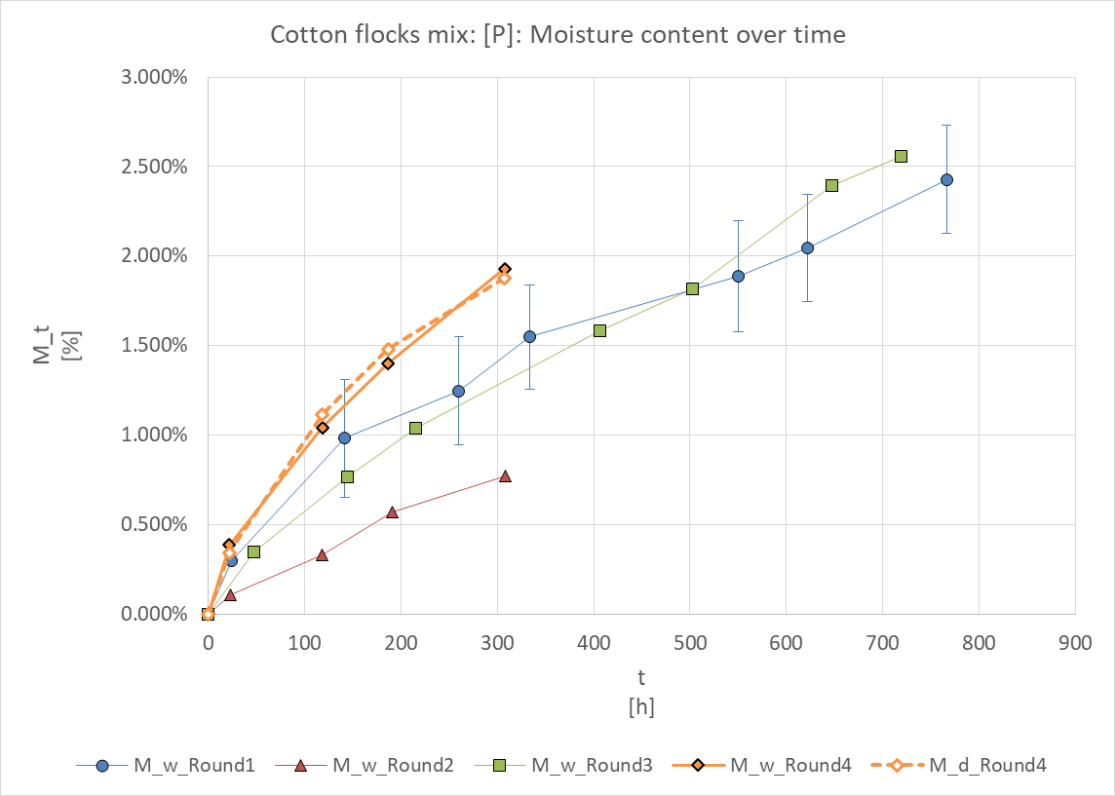

Figure 27: Line graph of the moisture content for various rounds of permeability testing of cotton flocks

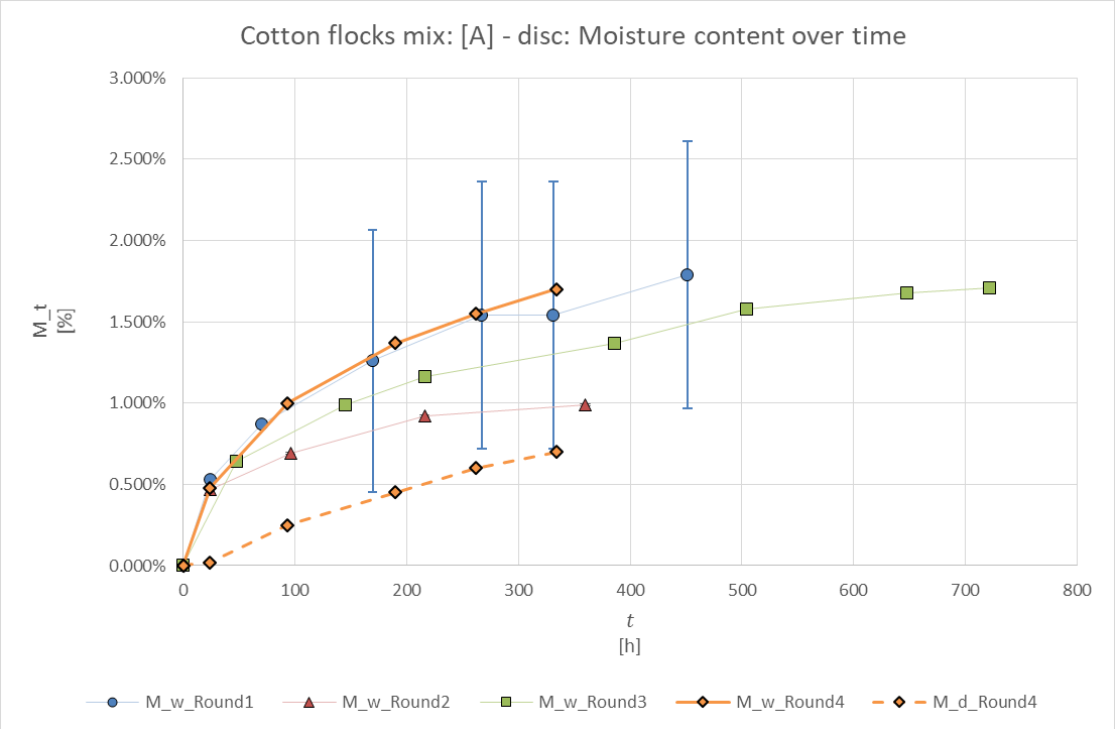

Figure 28: Line graph of the moisture content for various rounds of absorption testing of cotton flocks

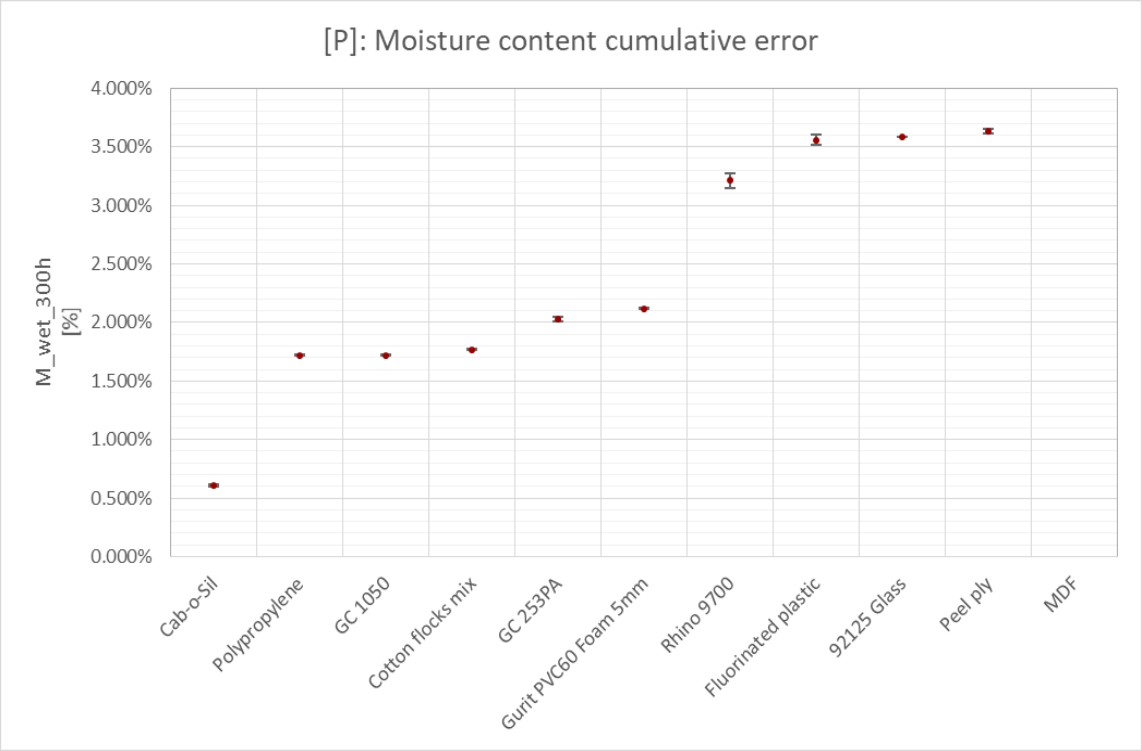

Figure 29: Cumulative error on moisture content of wet permeability samples is minimal after first round testing.

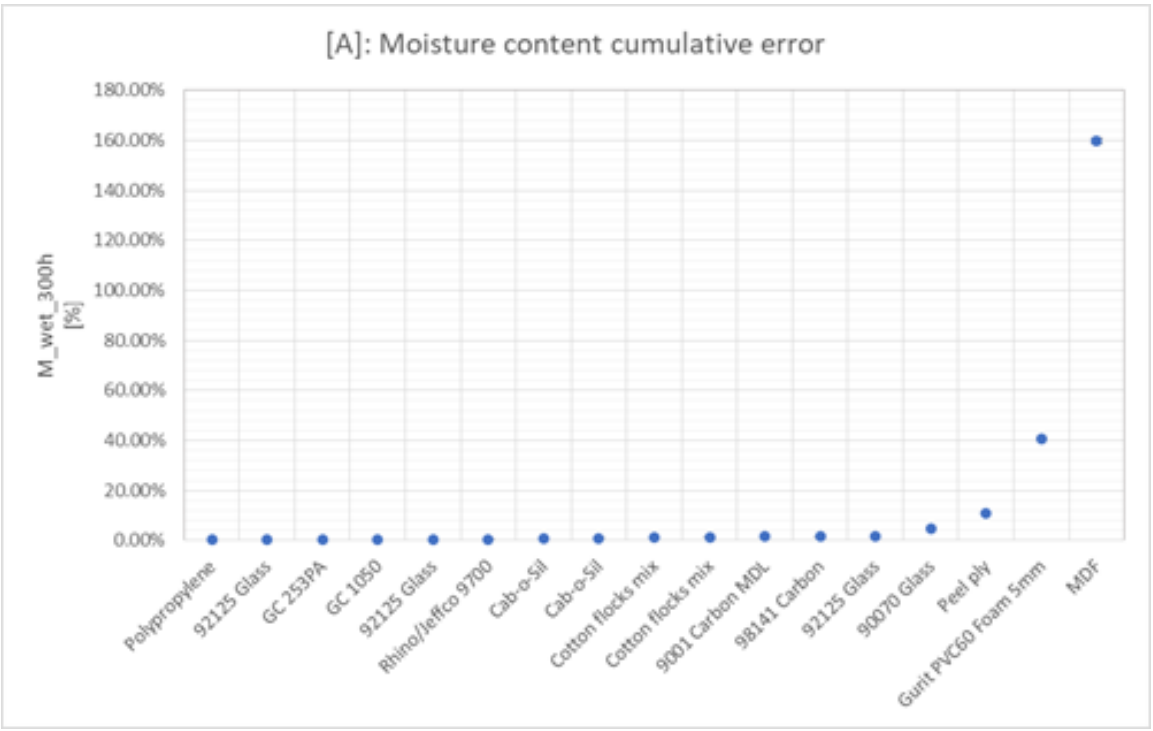

Figure 30: Cumulative error on moisture content of wet absorption samples is minimal after first round testing

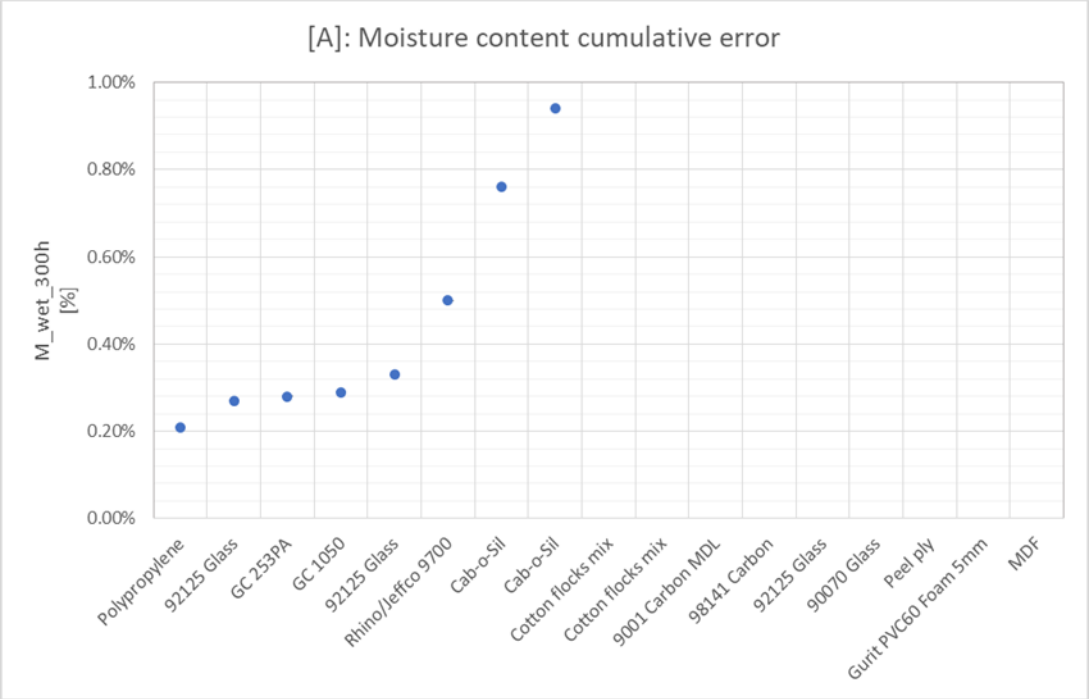

Figure 31: Cumulative error on moisture content of wet absorption samples is shown to be minimal after first round testing even on low (<1%) moisture content values

5.3.3 Change in thickness

The change in thickness of absorption samples was less than the measurement uncertainty in several instances. This meant that any potential tendencies noted could not be definitively based on the measurements. Figure 32 shows that nearly half (8 out of 17) of the samples had a larger propagated measurement uncertainty than the thickness variation itself. This large degree of uncertainty can be ascribed to surface hardness of the samples. Soft samples were hard to measure consistently with a calliper-type micrometer that requires firm contact. The relatively low resolution of micrometer used (0.005mm) for measuring maximum deformation, Δt_{max}, of only 0.02 mm. A verdict on the material(s) causing the deformation in the wing tip could not be made with such a high level of measurement uncertainty.

As for permeability samples, their change in thickness was primarily as a result of the MDF in the substrate swelling. Swelling of MDF was particularly evident when it did not have any 92125 Glass on-top of it (as shown in Figure 33).

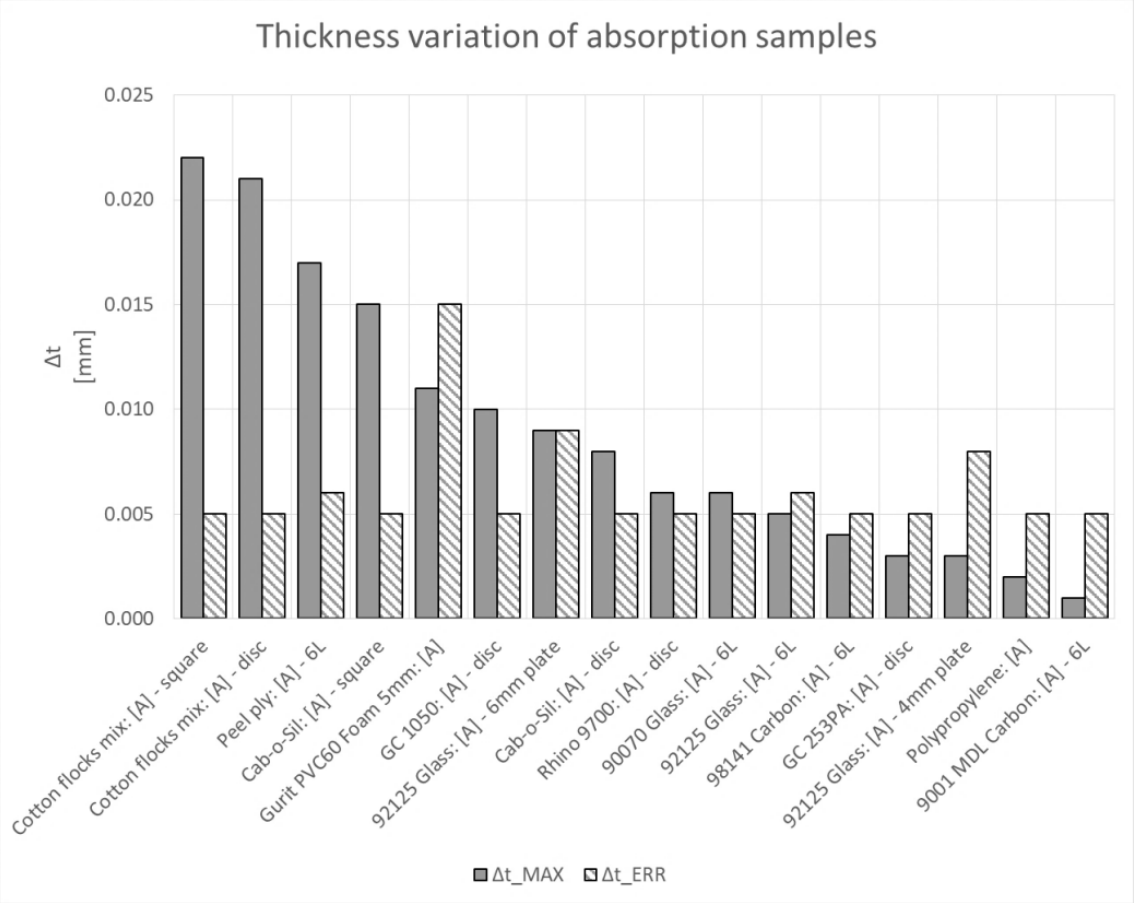

Figure 32: Maximum thickness variation (Δt_MAX) in absorption samples along with the associated measurement uncertainty (Δt_ERR)

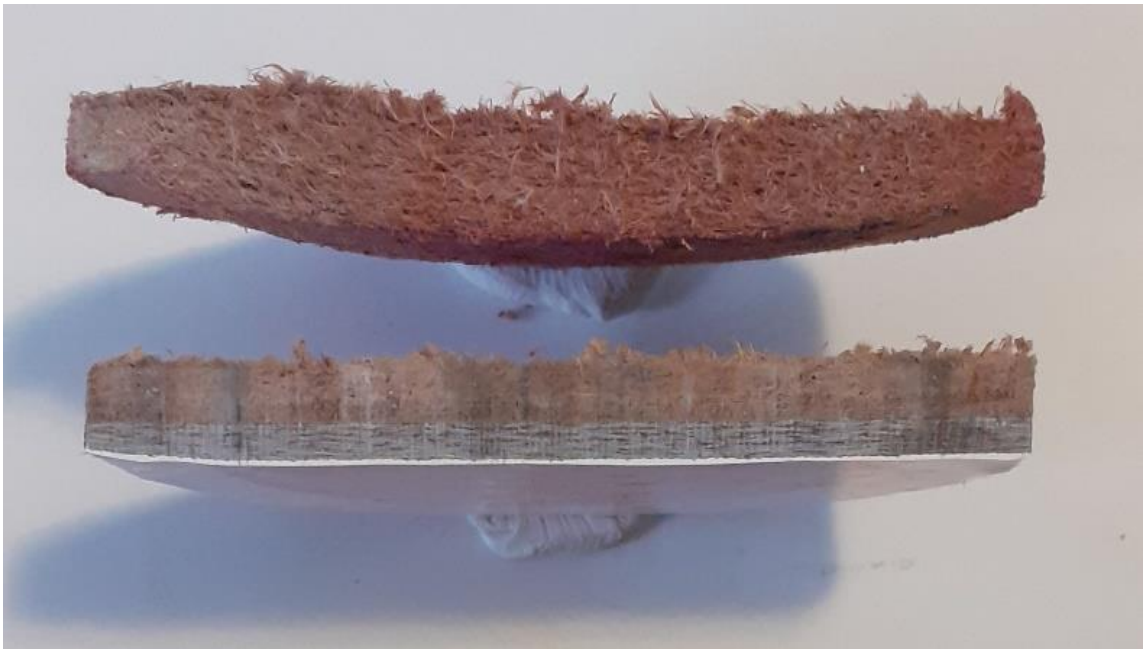

Figure 33: Visible swelling in MDF versus a substrate with GC1 050 coating (bottom) and minimal swelling

5.4 Material category results

5.4.1 Fillers and coatings

In Figure 34 the values of the permeability criteria parameters are shown in the stacked column graph. When considering the parameters, it is evident that most of the materials are closely matched based on β-values. The $\alpha\gamma$-Score only helped differentiate that fluorinated plastic is the only material that is scored negatively. Three of the materials received the no verdict based on the $\alpha\gamma$-values. Moreover, absorption criteria parameters (shown in the graph in Figure 35) were considered to assist in distinguishing the materials that performed similarly in terms of permeability scoring.

The two gelcoats (GC1 050 and GC 253PA) returned near-identical parameter values which were the lowest in this category – making them the two most suitable materials as for keeping the sandwich structure shielded from moisture. However, in the specification sheet of GC 253PA (Scott Bader, 2012), the manufacturer does not recommend applying the coating where it will be subject to continuous immersion in water (like in a ballast tank). No such recommendations against usage in aqueous environments is made in the product data sheet of GC 1 050 (SikaBiresin®, 2020).

The filler materials, Cab-O-Sil® and cotton flocks yielded similar results on the permeability front, but CoS clearly showed lower absorption in terms of the criteria parameters. The moisture content of CoS was 0.940±0.005% versus 1.430±0.005% in Cotton Flocks. Based on the substantially lower absorption values of CoS, it is the better of the two fillers and also one of the top three materials in this category.

A comparison of the two materials waterproofing the largest portions of the ballast tank shows that Rhino 9700 outperforms fluorinated plastic with substantially better permeability characteristics. Fluorinated plastic was not tested in the absorption experiments. A piece of fluorinated plastic of similar length and breadth as the largest absorption sample was too thin and fragile to dry and measure properly. It would also be very light. It would have been about 0.20g lighter than the already-very-light PVC60 (which had an issue due to its lightness). Secondly, making fluorinated plastic several layers thick, would make distinct strata of epoxy between each layer as the plastic would not act the same as fibre reinforcement would in a normal polymer-matrix composite. Essentially, in an absorption test of a multi-layered fluorinated plastic sample, the additional inter-laminar epoxy could greatly distort the representation of the characteristics of a single-ply fluorinated plastic sheet in real-world application. Making other coatings multiple layers thick is often standard practice, but not so with fluorinated plastic. Nevertheless, samples with fluorinated plastic still got a worse (higher) $\Pi_{[P]}$ rank score than both uncoated 92125 Glass and samples coated with peel ply (as previously shown by the rank-scores in Figure 26). Between Rhino 9700 and peel ply, the former is likely to provide better water resistance based on its low absorption characteristics – especially compared to peel ply's absorption which is the highest in this category.

In Figure 35 it can be seen that CoS and cotton flocks have error bars. The error bars in this instance are not indicative of uncertainty but of minimum values of the differently shaped samples (disc and square, as disclosed in Section 3.6.2). These very small error bars show that for a given material, the variance in both M and θ-values is barely affected by the difference in surface-to-area ratio. This further implies that inter-variant samples dissimilar physical dimensions did not have a significant effect on the percentage moisture gained – in CoS and cotton flocks samples at least. Materials don't all share this tendency as will be shown in the next section of this article.

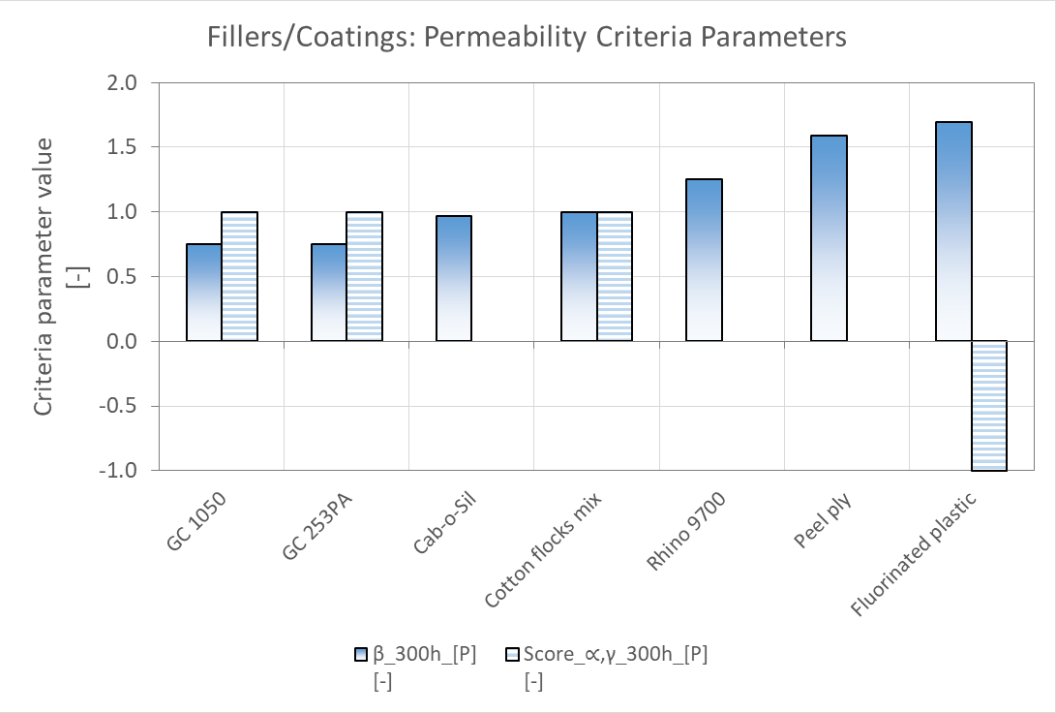

Figure 34: Values of permeability criteria parameters of filler and coating materials

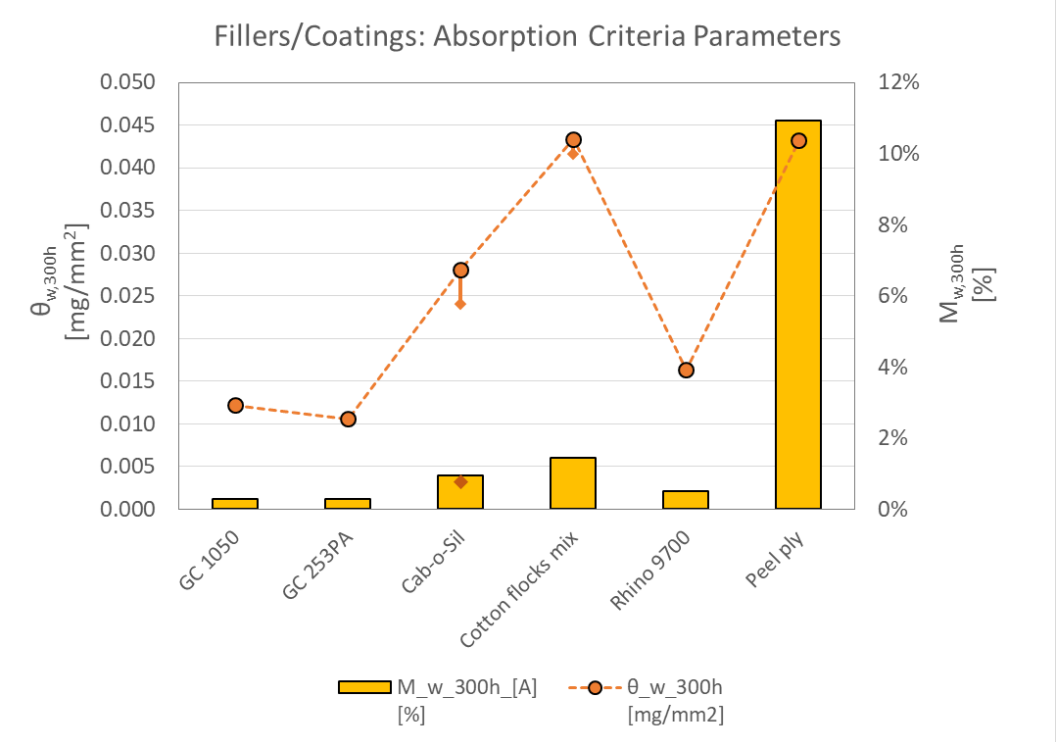

Figure 35: Values of absorption criteria parameters of filler and coating materials

5.4.2 Polymer-matrix composites and foam

Since the PMC samples aren't meant to offer permeability resistance, it was of greater interest to determine which material in the sandwich structure absorbs the most moisture, once moisture permeates through the outer layer of coatings and/or fillers. It is however unusual that the PMCs exhibit lower absorption than some fillers and coatings.

In this category, the carbon fibre samples displayed the lowest absorption as shown in Figure 36. Sample composition calculations determined that 9001 Carbon MDL samples contain less epoxy than 98141 Carbon (see Table 12). Since carbon fibre reinforcement doesn't absorb moisture, but rather the epoxy in the matrix (Ryan *et al.*, 2009) 9001 Carbon MDL absorbs less than 98141 Carbon.

Glass fibres are more susceptible to environmental effects and degradation than carbon fibre (Karbhari & Zhang, 2003; Tsenoglou *et al.*, 2006). As a result, for the same number of layers (six), carbon fibre samples absorbed less than fibreglass variants. In a similar manner to 9001 and 98141 Carbon, 90070 Glass laminate had more epoxy than 92125 Glass laminate and consequently, lower absorption parameter values. The negative error-bars at 92125 Glass's θ and $M_{w,300h}$-values belong to the 6mm-thick variant of 92125 Glass. This signifies that due to a lower area-to-volume ratio (see Figure 36) thicker samples do offer substantially lower absorption characteristics in terms of moisture content (M_w) and mass gain per unit area (θ_w). Table 13 lists the characteristics of the different 92125 Glass variants.

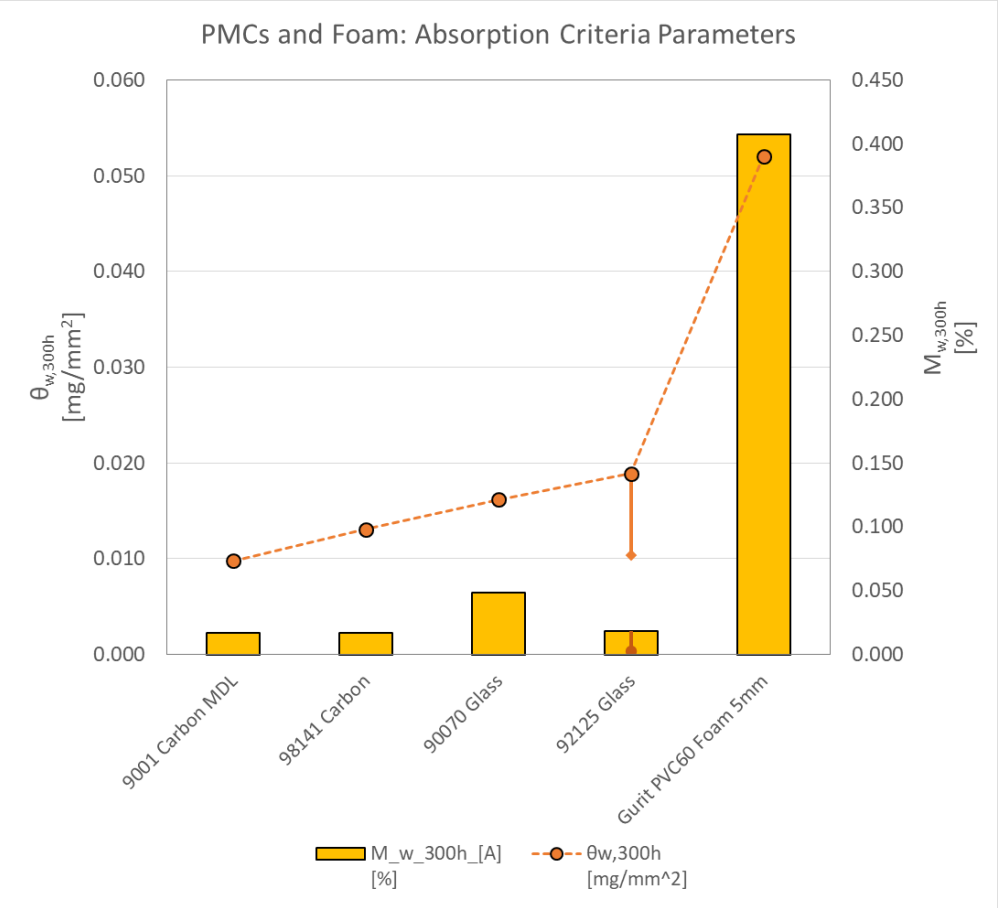

Figure 36: Values of absorption criteria parameters of PMCs and foam

Table 12: Six layered laminates characteristics and epoxy content

Material	Layers	m_0 [g]	L [mm]	W [mm]	gsm [g/m²]	$m_{0,fabric}$ [g]	$m_{0,epoxy}$ [g]	$M_{w,300h}$ [%]	$\Delta m_{w,300h}$ [g]
9001 MDL Carbon	6	4.178	64	54	140	2.903	1.275	1.67%	0.0698
98141 Carbon	6	5.959	61	61	200	4.465	1.494	1.70%	0.1013
92125 Glass	6	7.946	68	54	280	6.169	1.777	1.82%	0.1446
90070 Glass	6	2.933	69	63	80	2.087	0.847	4.88%	0.1431

Table 13: Characteristics of 92125 Glass variants

Variant	m_0 [g]	h [mm]	A [$\times 10^3$ mm^2]	A-V [mm^2/mm^3]	$\Delta m_{w,300h}$ [g]	$M_{w,300h}$ [%]
6L	7.95	1.27	7.65	1.64	0.14	1.82%
4mm	29.18	4.12	9.32	0.55	0.10	0.33%
6mm	40.51	5.69	9.60	0.41	0.11	0.27%

Furthest to the absorptive-side of the graph is PVC60 foam with much higher M_w and θ_w-values than the PMCs. This implies that the foam probably retains the largest amount of water in the sandwich structure when water seeps in. Interestingly, the foam achieved a better (lower) than average permeability rank score ($\Pi_{[P]}$) – even lower than CoS. Examination of PVC60 permeability samples showed no colourant residue beyond the first layer or two of exposed pores near the surface (refer to Figure 37 and Figure 38) – indicating that water penetration is shallow but the amount of water adhering to the samples surface is large. One reason that this relatively small amount of surface water causes such a high mass increase ($M_{w,300h} = 40.72\%$) in absorption testing is because of the very low mass of foam samples (±0.91 g). The PVC60's mass gain of 0.37 g remains among the highest of the absorption values measured, nonetheless (refer back to Table 7).

In Figure 37 it can be seen that there is a clear area around the circumference of the PVC60 sample where the seal was located in the test rig. This clear area shows that minimal, if any, liquid seeped passed this sample's seal. The effectivity of the seal of other sample types was also judged by checking if the seal contact area was devoid of colourant residue. The side profile of the foam sample in Figure 38 does show some dark lines or strips below the top cell layers, but these are not from colouring residue. When sawing the sample in half, friction and heat build-up caused these slight burn marks.

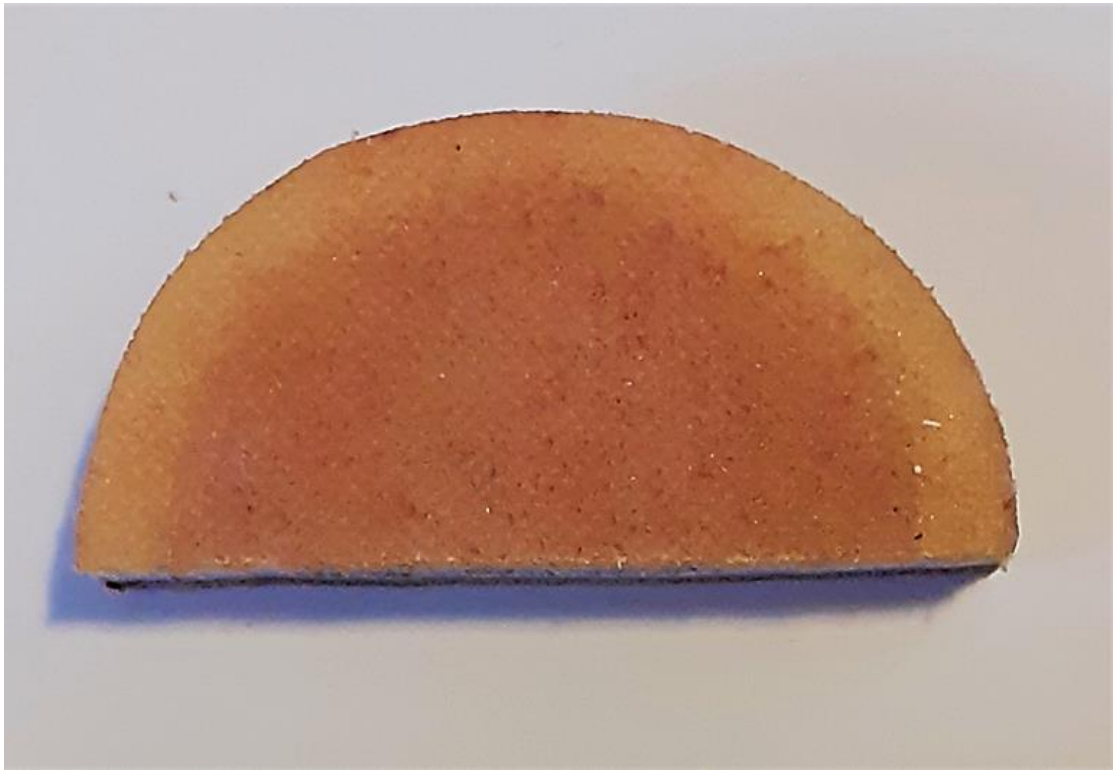

Figure 37: Top view of a cut PVC60 permeability sample with red residue from the coloured water showing where water accumulated on the exposed surface

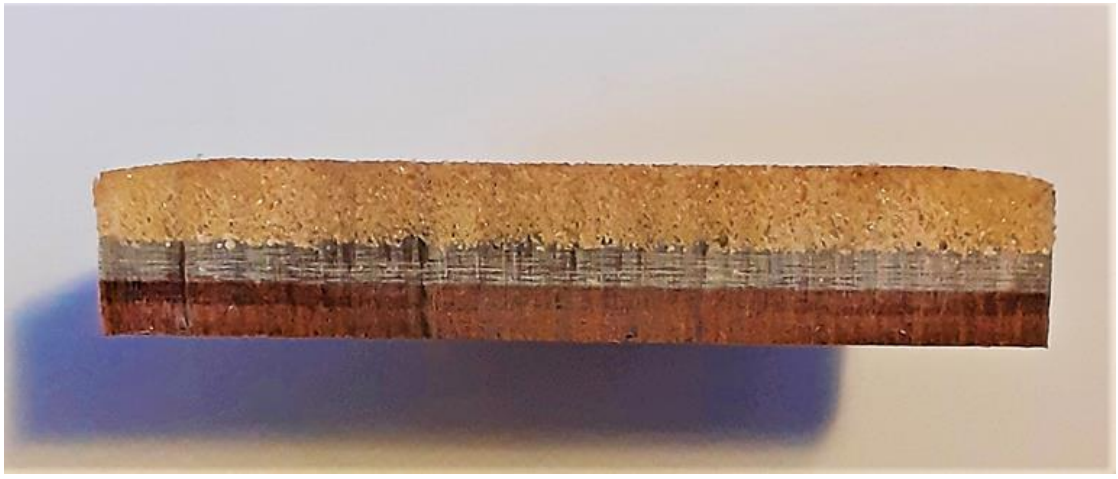

Figure 38: Side profile view of a cut PVC60 permeability sample showing no residue of the coloured water beyond the surface

5.5 Validation of results

The absorption data from literature was used to validate the experimental results. Refer to Table 1 in Section 2.2.3 for more details. Table 14 lists the materials for which absorption values could be found in literature and specification sheets. The duration of the literature study test listed in the column furthest to the right is the time at which the experimental value listed in the second-from-left column was interpolated.

It can be seen that majority of the experimentally determined values ($M_{w,EXP,t}$) correspond well with those from external studies or specification sheets ($M_{w,LIT,t}$). The one obvious non-conforming value is that of 90070 Glass (4.88%) which doesn't match closely with the E-glass with vinyl ester resin (0.9%). This could mostly be attributed to the different matrix materials (vinyl ester resin vs thermosetting epoxy resin) being used and the different composition of the glass fibres found in E-glass and 90070 Glass. Data on a fibreglass material more similar to 90070 Glass could not found. The more minor variations in other materials can be ascribed to various factors such as approximation errors in interpolation or reading values off from graphs and differences in environmental conditions.

Table 14: Validation of experimental absorption values using values from external studies noted in the literature review

		Similar Type Material/ External Study of Test Material		
Test Material Name	**$M_{w,EXP,t}$ [%]**	**Name of Similar Material**	**$M_{w,LIT,t}$ [%]**	**t [h]**
Carbon 9001 MDL	0.9-1.2%[3]	Carbon fibre epoxy resin pre-preg	1.4%	-
Carbon 98141	0.8-1.2%	UD carbon with epoxy resin	0.8%	300
92125 Glass	0.27-1.8%	E-glass with vinylester resin	0.370%	288
90070 Glass	3.3-4.6%	E-glass with isophthalic polyester resin	0.9%	300
MDF	84-94%	Medium density fibre board (MDF)	80%	168
Polypropylene	0.02-0.11%	Polypropylene	0.01%	24
Rhino 9700	0.08-0.13%	Rhino 9700	<1%	24
Peel Ply	9-12%	Polyamide 6	9%	370

[3] Duration taken as 300 hours

5.6 Verification of results

The results displayed in this chapter were all the output of several steps of processing, mostly done semi-automatically by computing of values using various formulas duplicated in Microsoft Excel spreadsheets. This sub-section provides example calculations showing that the Excel inputs and formulas were done accurately and yield the same or very similar result to manual calculation of the same parameter. This aids in the verification that thoughtless mistakes were not made in the commands which were executed in the spreadsheets. The example variables to be manually computed for verification purposes are moisture content and its corresponding error, and then the rank-score of GC 253PA.

5.6.1 Moisture content and cumulative error

Since moisture content is a primary variable used as a measure of a sample's absorption and permeability, it was critical to know that the cumulative error on the calculated value was within reasonable limits. A manual calculation will now be done on the 95th percentile values of GC 253PA gelcoat absorption samples at 300 hours to validate that the semi-automated spreadsheet computations were done correctly.

Calculation of the cumulative error on the reported moisture content value is determined by looking at the equation for computing moisture content, namely

$$M = \frac{m_{300h} - m_0}{m_0}$$

This should be rewritten as

$$M = \frac{m_{300h}}{m_0} - 1$$

when applying cumulative error rules to avoid compensating errors (Taylor, 1997). The value of mass measurement uncertainty for GC 253PA's dry (m_0) and wet (m_t with $t > 0$) measurements was 0.0002 g for absorption testing. The materials moisture content was 0.27749%.

By the rule of cumulative error for division of correlated values, the error on M_{300h} is

$$\begin{aligned}\delta M_{300h,GC\ 253PA\ [\mathrm{A}]} &\approx \delta\left(\frac{m_{300h}-m_0}{m_0}\right)_{[\mathrm{A}]}\\ &= \left(\frac{m_{300h}}{m_0}-1\right)\cdot\left(\frac{\delta m_t}{m_t}+\frac{\delta m_0}{m_0}\right)\\ &= \left(\frac{10.9733}{10.9427}-1\right)\cdot\left(\frac{0.0002}{10.9733}+\frac{0.0002}{10.9427}\right)\\ &= (0.00279638\ldots)(0.00003650\ldots)\\ &= 1.0207\ldots\times 10^{-7}\ [gram\ moisture/gram\ material]\\ &\approx 0.00001\%\end{aligned}$$

Therefore, we have that

$$M_{300h,GC\ 253PA\ [\mathrm{A}]} = 0.27964 \pm 0.00001\ \%$$

This is the approximate equivalent of the automatically computed value reported to the second significant figure, namely

$$M_{300h,GC\ 253PA\ [\mathrm{A}]} = 0.28 \pm 0.00\ \%$$

However, it can be noted that there is a considerable difference in the fractional uncertainty. This manual calculation gives a value of approximately 0.004% but the value is listed as 0.007% in Table 11. This could be attributed to the fact that the automatically computed value of 0.007% included interpolation errors which would be very tedious to include in this manual calculation.

5.6.2 Rank-score calculation

An example calculation of the permeability rank score of GC 253PA will now be given to verify that the reported values in Section 5.4.1 are correct. Starting with (Eq 8) we have that

$$\begin{aligned}\beta_{300,GC\ 253\ PA:[\mathrm{P}]} &= \left(\frac{M_w}{M_d}\right)_{300,GC\ 253PA\ :\ [\mathrm{P}]}\\ &= \left(\frac{2.03}{2.70}\right)\\ &= 0.752\end{aligned}$$

This simple calculation yielded the same value reported in the graph in Figure 34, thus we can assume that the other values were also computed correctly. Comparing GC 353PA to other variants' scores shows that GC 253PA ranks 9th (see Table 15 and consequently has a 2β-Score of 18.

Table 15: Determining the β-Score of GC 253PA

Material	$\beta_{300h,\,[P]}$ [-]	2 × β-Score [-]
MDF	9.48	2.00
Fluorinated plastic	1.70	4.00
Peel ply	1.59	6.00
92125 Glass	1.51	8.00
Rhino 9700	1.25	10.00
Cotton flocks mix	0.99	12.00
Cab-o-Sil	0.97	14.00
Gurit PVC60 Foam 5mm	0.96	16.00
GC 253PA	0.75	18.00
GC 1050	0.75	20.00
Polypropylene	0.67	22.00

Next, we use (Eq 9)

$$\propto_{300,d,GC\ 253\ PA:\,[P]} = \left(\frac{\Delta m_{\text{GC 253PA: [P]}}}{\Delta m_{\text{92125 Glass: [P]}-\text{6L}}}\right)_{300,d}$$
$$= \left(\frac{0.409}{0.345}\right)$$
$$\approx 1.19$$

and then (Eq 10)

$$\gamma_{300,w,GC\ 253\ PA:[P]} = \left(\frac{\Delta m_{\text{GC 253PA: [P]}}}{\Delta m_{\text{92125 Glass: [P]}-\text{6L}}}\right)_{300,w}$$
$$= \left(\frac{0.31}{0.52}\right)$$
$$\approx 0.60$$

Since $\propto_{t,d,GC\ 253\ PA:\,[P]} > 1$ and $\gamma_{t,w,GC\ 253\ PA:[P]} < 1$, the verdict of GC 253PA having low water permeability (refer to Table 5 in Section 4.3), or in scoring terms,

$$\alpha\gamma\text{-}Score = 1$$

Using (Eq 23)

$$\Pi_{[P],\text{GC 253PA}} = \left(\frac{5}{11}\right)\left[24 - Y_{[P],\text{GC 253PA}}\right]$$

and then substituting (Eq 12) for Y, it can be found that

$$\begin{aligned}\Pi_{[P],GC\ 253\ PA} &= \left(\frac{5}{11}\right)[24 - (2\beta\text{-}Score\ + \alpha\gamma\text{-}Score)] \\ &= \left(\frac{5}{11}\right)[24 - \big((18) + (1)\big) \\ &\approx 2.3\end{aligned}$$

As before, this correlates with the value of 2.3 reported in the graph in Figure 26.

6 CONCLUSIONS AND RECOMMENDATIONS

In this study the absorption and permeability characteristics of various composite materials were determined with a unique gravimetric moisture-measuring technique. The quantitative data obtained from the various rounds of experimentation alone was not sufficient for comparing characteristics of the different materials. The development of criteria and relative scoring allowed for a more complete comparison of material characteristics. Comparing non-criteria parameters (such as initial mass, area-to-volume ratio, etc.) remained essential to the understanding of the results and, as such, should be used in conjunction with the criteria rankings.

In this experimental investigation it was found that the best coatings are jointly the two variants of gelcoat, GC253PA and G 1 050, with low permeability and low absorption per unit area. Cab-O-Sil® and Cotton Flocks fillers had similarly low permeability and low absorption, but were rated lower than the gelcoats. The lowest-rated coating materials currently in use in the ballast tank region were Rhino 9700 and fluorinated plastic.

Samples made of carbon fibre fabric absorbed less moisture than fibreglass samples. Finally, fibreglass had better resistance to water ingress in terms of quantity than PVC60 Foam. PVC60 Foam was thus the coated material that absorbed the most water per unit of material mass.

This study met two of the three objectives specified in the beginning of this study. Firstly, quantitative data on characteristics pertaining to water resistance and absorption was measured. Secondly, data was processed into a comparative format so as to predict which materials performed the best in their respective functional categories. The study only fell short in measuring deformation accurately due to instrumentation limitations – but this could be remedied if one had prior knowledge of the high measuring resolution required and was provided with access to correct instrumentation or the funding for it.

It has been shown that this method of relative comparison of qualitative data can yield results that can be supported by additional factors and sources. There remains room for refinement and improvement of the methodology. Improvements to the experimental method could include:

- Manufacture the highly absorbent component of the material as a separate entity from the test material component in the permeability test. This will allow for isolated analysis of mass gain of the two individual components.

- Use a non-contact measuring instrumentation with resolution of less than 0.1 μm. This higher resolution will help keep the measurement uncertainty within acceptable limits.

APPENDIX A: Sample calculation of mass measurement uncertainty values – Rhino absorption samples

a) <u>WMMA value:</u>

1) Determine average of the first mass and second mass

$$\begin{aligned}\overline{m}_{Rhino\ [A]:WMMA} &= \frac{(m_0 + m_1)}{N} \\ &= \frac{9.7091 + 9.7090}{2} \\ &= 9.70905\ [\mathrm{g}]\end{aligned}$$

2) Compute the variance

$$\begin{aligned}Var_{Rhino\ [A]:WMMA} &= \frac{(\overline{m} - m_0)^2 + (\overline{m} - m_1)^2}{N - 1} \\ &= \frac{(9.70905\ - 9.7091)^2 + (9.70905\ - 9.7090)^2}{2 - 1} \\ &= 5 \times 10^{-9}\end{aligned}$$

3) Thirdly, the standard deviation (σ_m) could be calculated to be

$$\begin{aligned}\sigma_{m,Rhino\ [A]:WMMA} &= \sqrt{Var_{Rhino\ [A]:WMMA}} \\ &= \sqrt{5 \times 10^{-9}} \\ &= 7.07\ldots \times 10^{-5}\end{aligned}$$

4) Lastly, the wet mass measurement uncertainty of Rhino absorption samples was found to be

$$\begin{aligned}\delta m_{Rhino\ [A]:WMMA} &= 2\sigma_{m,Rhino\ [A]:WMMA} \\ &= 0.0001414\ldots \\ &\approx 0.0001\ [\mathrm{g}]\end{aligned}$$

b) DMMA value:

1) Determine average of the first mass and second mass

$$\bar{m}_{Rhino\ [A]:DMMA} = \frac{(m_0 + m_1)}{N}$$
$$= \frac{9.5229 + 9.5232 + 9.5234 + 9.5231 + 9.5231 + 9.5234 + 9.5232 + 9.5234 + 9.5230}{9}$$
$$\approx 9.52319\ [\text{g}]$$

2) Compute the variance

$$Var_{Rhino\ [A]:DMMA} = \frac{(\bar{m} - m_0)^2 + (\bar{m} - m_1)^2 + \cdots}{N - 1}$$
$$= \frac{(9.52319\ \ - 9.7091)^2 + (9.52319\ \ - 9.5232)^2 + \cdots}{9 - 1}$$
$$= 2.987 \ldots \ldots \times 10^{-8}$$

3) Thirdly, the standard deviation (σ_m) could be calculated to be

$$\sigma_{m,Rhino\ [A]:DMMA} = \sqrt{Var_{Rhino\ [A]:DMMA}}$$
$$= \sqrt{2.987 \ldots \ldots \times 10^{-8}}$$
$$= 0.000172 \ldots\ [\text{g}]$$

4) Lastly, the dry mass measurement uncertainty of Rhino absorption samples was found to be

$$\delta m_{Rhino\ [A]:DMMA} = 2\sigma_{m,Rhino\ [A]:DMMA}$$
$$= 2(0.000172 \ldots)$$
$$\approx 0.0003[\text{g}]$$

REFERENCE LIST

Airex AG 2010. Airex Baltek: Additional technical data of Airex C70.

Alfrey Jr, T., Gurnee, E. & Lloyd, W. Diffusion in glassy polymers. Journal of Polymer Science Part C: Polymer Symposia, 1966. Wiley Online Library, 249-261.

Anatoly, C., Pavel, Z., Tatiana, C., Alexei, R. & Svetlana, Z. 2020. Water vapor permeability through porous polymeric membranes with various hydrophilicity as synthetic and natural barriers. *Polymers,* 12**,** 282.

Antoon, M. & Koenig, J. 1980. The structure and moisture stability of the matrix phase in glass-reinforced epoxy composites. *Journal of Macromolecular Science—Reviews in Macromolecular Chemistry,* 19**,** 135-173.

Apicella, A., Migliaresi, C., Nicolais, L., Iaccarino, L. & Roccotelli, S. 1983. The water ageing of unsaturated polyester-based composites: influence of resin chemical structure. *Composites,* 14**,** 387-392.

Arnold, C., Korkees, F. & Alston, S. The long-term water absorption and desorption behaviour of carbon-fibre/epoxy composites. Proceeding of ECCM, 2012.

Beaman, R. G. & Cramer, F. B. 1956. Polymer characterization: A typical copolyamide system. *Journal of Polymer Science,* 21**,** 223-235.

Boermans, L. & Selen, H. 1981. On the design of some airfoils for sailplane application. *Technical Soaring.*

Bonniau, P. & Bunsell, A. 1981. Water absorption by glass fibre reinforced epoxy resin. *Composite structures.* Springer.

Bosman, J. & Jonker, A. 2019. Water Absorption in Glider Wings [personal communication].

Bumgarner, C. 2003. Blisters & Laminate Hydrolysis. *Best of the Bay Chesapeake Bay Magazine.* Zahniser's Yachting Center.

Choudalakis, G. & Gotsis, A. D. 2012a. Free volume and mass transport in polymer nanocomposites. *Current opinion in colloid & interface science,* 17**,** 132-140.

Choudalakis, G. & Gotsis, A. D. 2012b. Free volume and mass transport in polymer nanocomposites. *Current opinion in colloid & interface science.* Elsevier.

Clément, J.-M. 2006. Sailplane Design and Record Flights. *Technical Soaring,* 30**,** 112-118.

Commission, E. 2012. Regulation (EC) No 231/2012 of 9 March 2012 laying down specifications for food additives listed in Annexes II and III to Regulation (EC) No 1333/2008 of the European Parliament and of the Council. *Official Journal of the European Communities*.

Deng, H., Reynolds, C., Cabrera, N., Barkoula, N.-M., Alcock, B. & Peijs, T. 2010. The water absorption behaviour of all-polypropylene composites and its effect on mechanical properties. *Composites Part B: Engineering,* 41**,** 268-275.

Derrien, K. & Gilormini, P. 2009. The effect of moisture-induced swelling on the absorption capacity of transversely isotropic elastic polymer–matrix composites. *International Journal of Solids and Structures,* 46**,** 1547 - 1553.

DG Flugzeugbau. 2017. *The DG-1001 Trim Box* [Online]. Available: https://www.dg-flugzeugbau.de/en/library/dg-trim-box [Accessed 15 January 2020].

Eisele, M. 2019. 18m tips [e-mail]: 11 Nov. 2019.

Enderby, J. 1955. Water absorption by polymers. *Transactions of the Faraday Society,* 51**,** 106-116.

Ensinger Plastics 2021. Dimensionally stable plastics.

Federal Aviation Administration 2013. Glider Flying Handbook.

Giddy, J. n/a. *Water Ballast Issues: Leak Proofing Integral Tanks* [Online]. Schempp-Hirth Standard Cirrus. Available: http://www.standardcirrus.org/WaterBallast.php [Accessed 12 September 2020].

Giguere, J. S. 2000a. Damage mechanisms and non-destructive testing in the case of water ingress in CF-18 flight control surfaces.

Giguere, J. S. Damage mechanisms and non-destructive testing in the case of water ingress in CF-18 flight control surfaces. 2000b.

Gopi, S., Loganathan, G. B., Sekar, B. K., Krishnamoorthy, R. K., Sekaran, V. & Mohan, A. R. 2019. Influence of water absorption on glass fibre reinforced IPN composite pipes. *Polímeros,* 29.

Gopu, J. S. 2012a. A Review Of Mechanisms And Fracture Mechanics Of Moisture Ingress In Composite Systems. *Theses and dissertations*.

Gopu, J. S. 2012b. A Review Of Mechanisms And Fracture Mechanics Of Moisture Ingress In Composite Systems. *Theses and dissertations.*

Grammatikos, S. A., Ball, R. J., Evernden, M. & Jones, R. G. 2018. Impedance spectroscopy as a tool for moisture uptake monitoring in construction composites during service. *Composites Part A: Applied Science and Manufacturing,* 105**,** 108-117.

Grammatikos, S. A., Zafari, B., Evernden, M. C., Mottram, J. T. & Mitchels, J. M. 2015. Moisture uptake characteristics of a pultruded fibre reinforced polymer flat sheet subjected to hot/wet aging. *Polymer Degradation and Stability,* 121**,** 407-419.

Grassini, S., Corbellini, S., Angelini, E., Ferraris, F. & Parvis, M. 2014. Low-cost impedance spectroscopy system based on a logarithmic amplifier. *IEEE Transactions on Instrumentation and Measurement,* 64**,** 1110-1117.

Grundling, G. 2019. Water Absorption in Glider Wings [personal interview].

Gurit. 2021. *Guide to Composites* [Online]. Available: https://www.gurit.com/-/media/Gurit/Datasheets/guide-to-composites.pdf [Accessed 26 March 2021].

Heydari, A. & Sheibani, H. 2015. Fabrication of poly (β-cyclodextrin-co-citric acid)/bentonite clay nanocomposite hydrogel: thermal and absorption properties. *RSC advances,* 5**,** 82438-82449.

Hopfenberg, H. & Stannett, V. 1973. The Physics of glassy polymers. *Appl. Sci. Publishers, London*.

Hsieh, G., Edwards, D., Ford, S., Hwang, J.-H., Shane, J., Garboczi, E. & Mason, T. O. 1995. Experimental limitations in impedance spectroscopy of materials systems. *MRS Online Proceedings Library (OPL),* 411.

ISO 2004. International vocabulary of basic and general terms in metrology (VIM). *International Organization for Standardization,* 2004**,** 09-14.

John, M., Schlimper, R., Rinker, M., Wagner, T., Roth, A. & Schäuble, R. 2011. Long-term durability of CFRP foam core sandwich structures. *CEAS Aeronautical Journal.* Springer.

Karbhari, V. & Zhang, S. 2003. E-glass/vinylester composites in aqueous environments–I: experimental results. *Applied Composite Materials,* 10**,** 19-48.

Keller, P. E. & Kouzes, R. T. 2017. Water vapor permeation in plastics. Pacific Northwest National Lab.(PNNL), Richland, WA (United States).

Kotze, A. 2019. Water Absorption in Glider Wings [personal communication].

Krzyżak, A., Mazur, M., Gajewski, M., Drozd, K., Komorek, A. & Przybyłek, P. 2016. Sandwich structured composites for aeronautics: methods of manufacturing affecting some mechanical properties. *International Journal of Aerospace Engineering,* 2016.

LaPlante, G., Marble, A. E., MacMillan, B., Lee-Sullivan, P., Colpitts, B. G. & Balcom, B. J. 2005. Detection of water ingress in composite sandwich structures: a magnetic resonance approach. *NDT & E International.* Elsevier.

Li, M. 2000. Temperature and moisture effects on composite materials for wind turbine blades. Montana State University.

Lide, D. R. 1995. *CRC handbook of chemistry and physics: a ready-reference book of chemical and physical data*, CRC press.

López, C. C., Lefebvre, X., Brusselle-Dupend, N., Klopffer, M.-H., Cangémi, L., Castagnet, S. & Grandidier, J.-C. 2016. Effect of porosity and hydrostatic pressure on water absorption in a semicrystalline fluoropolymer. *Journal of materials science,* 51**,** 3750-3761.

Ltd, N. A. P. 2019. Selling Specification: Rectified Extra Neutral Ethanol– C2H5OH.

Manujesh, B. J., Rao, V. & Aan, M. P. S. 2014. Moisture absorption and mechanical degradation studies of polyurethane foam cored E-glass-reinforced vinyl-ester sandwich composites. *Journal of Reinforced Plastics and Composites.* SAGE Publications Sage UK: London, England.

Maxwell, A. S., Broughton, W. R., Dean, G. D. & Sims, G. D. 2005. Review of accelerated ageing methods and lifetime prediction techniques for polymeric materials.

McGrath, P. F. 2000. Water Permeability vs Waterproof. *ASCE Met Section Construction Group, Cooper Union Student Chapter***,** 1-8.

McMurry, J. & Simanek, E. 2003. Fundamentals of organic chemistry. *Thomson Brooks/Cole, California*.

Monson, L., Braunwarth, M. & Extrand, C. 2008. Moisture absorption by various polyamides and their associated dimensional changes. *Journal of Applied Polymer Science,* 107**,** 355-363.

Munoz, E. & García-Manrique, J. A. 2015. Water absorption behaviour and its effect on the mechanical properties of flax fibre reinforced bioepoxy composites. *International journal of polymer science,* 2015.

Newill, J. R., McKnight, S. H., Hoppel, C. P. & Cooper, G. R. Effects of Coatings on Moisture Absorption in Composite Materials. 1999.

NTP 1992. National Toxicology Program Chemical Repository Database. *Research Triangle Park (NC): US Department of Health and Human Services, National Institutes of Health, National Toxicology Program*.

Özek, H. Z. 2018. Development of waterproof breathable coatings and laminates. *Waterproof and Water Repellent Textiles and Clothing.* Elsevier.

Park, G. S. & Crank, J. 1968. Diffusion in polymers.

Raghavalu Thirumalai, D. P., Løgstrup Andersen, T. & Lystrup, A. 2011. Influence of moisture absorption on properties of fiber reinforced polyamide 6 composites. DEStech Publications.

Rhino Linings. 2020. *Rhino 9700 Novolac* [Online]. Available: https://www.rhinoflooringofstmarys.com/products/rhino-9700/ [Accessed 13 Feb 2020].

Rogers, C. 1965. Physics and chemistry of the organic solid state. *Vol. edited by D. Fox,. MM Labes, A. Weissberger, Interscience, New York*.

Ryan, J., Adams, R. & Brown, S. Moisture ingress effect on properties of CFRP. Proceedings of the 17th International Conference on Composite Materials (ICCM'09), 2009.

Scott Bader 2012. CRYSTIC GELCOAT 253PA. 3 ed.

Shirangi, M. & Michel, B. 2010. Mechanism of moisture diffusion, hygroscopic swelling, and adhesion degradation in epoxy molding compounds. *Moisture sensitivity of plastic packages of IC Devices.* Springer.

SikaBiresin® 2020. Product Data Sheet: SikaBiresin® GC050 (GC1 050). *In:* RESINS, S. A. (ed.).

Sterling Plastics. 2012. *Polypropylene (Co-Polymer) - PPC* [Online]. Sterling Plastics, Inc. Available: http://sterlingplasticsinc.com/materials/polypropylene-co-polymer-ppc/ [Accessed 4 September 2020].

Suh, D.-W., Ku, M.-K., Nam, J.-D., Kim, B.-S. & Yoon, S.-C. 2001. Equilibrium water uptake of epoxy/carbon fiber composites in hygrothermal environmental conditions. *Journal of Composite materials,* 35**,** 264-278.

Surathi, P. & Karbhari, V. M. 2006. Hygrothermal effects on durability and moisture kinetics of fiber-reinforced polymer composites. California. Dept. of Transportation. Division of Engineering Services.

Taylor, J. 1997. *Introduction to error analysis, the study of uncertainties in physical measurements*.

Tsenoglou, C. J., Pavlidou, S. & Papaspyrides, C. D. 2006. Evaluation of interfacial relaxation due to water absorption in fiber–polymer composites. *Composites science and technology,* 66**,** 2855-2864.

Tucker, W. C., Lee, S.-B. & Rockett, T. 1993. The effects of pressure on water transport in polymers. *Journal of composite materials,* 27**,** 756-763.

Tukey, J. W. 1977. *Exploratory data analysis*, Reading, Mass.

Weitsman, Y. 1991. Moisture in composites: sorption and damage. *Composite Materials Series.* Elsevier.

West, J. 2021. What Could Affect the Rate of Diffusion of a Molecule Through a Membrane? Available: https://sciencing.com/could-affect-rate-diffusion-molecule-through-membrane-7994.html [Accessed 4 February 2021].

Wong, K. J. 2013. *Moisture absorption characteristics and effects on mechanical behaviour of carbon/epoxy composite: Application to bonded patch repairs of composite structures.* Dijon.

Xu, W., Winistorfer, P. M. & Moschler, W. W. 1996. A procedure to determine water absorption distribution in wood composite panels. *Wood and fiber science,* 28**,** 286-294.

Zarski, A., Bajer, K., Raszkowska-Kaczor, A., Rogacz, D., Zarska, S. & Kapusniak, J. 2020. From high oleic vegetable oils to hydrophobic starch derivatives: II. Physicochemical, processing and environmental properties. *Carbohydrate Polymers,* 243**,** 116499.

Zhai, Z., Feng, L., Liu, Z. & Li, G. 2016. Water absorption test for carbon fiber epoxy resin composite based on electrical resistance. *Polymer Testing,* 56**,** 394-397.